



Luo, M., Shi, G. R., Hu, S., Benton, M. J., Chen, Z. Q., Huang, J., ... Wen, W. (2017). Early Middle Triassic trace fossils from the Luoping Biota, southwestern China: Evidence of recovery from mass extinction. *Palaeogeography, Palaeoclimatology, Palaeoecology*.  
<https://doi.org/10.1016/j.palaeo.2017.11.028>

Peer reviewed version

License (if available):  
CC BY-NC-ND

Link to published version (if available):  
[10.1016/j.palaeo.2017.11.028](https://doi.org/10.1016/j.palaeo.2017.11.028)

[Link to publication record in Explore Bristol Research](#)  
PDF-document

This is the author accepted manuscript (AAM). The final published version (version of record) is available online via Elsevier at <https://www.sciencedirect.com/science/article/pii/S0031018217305254> . Please refer to any applicable terms of use of the publisher.

## **University of Bristol - Explore Bristol Research**

### **General rights**

This document is made available in accordance with publisher policies. Please cite only the published version using the reference above. Full terms of use are available:  
<http://www.bristol.ac.uk/pure/about/ebr-terms>

1 **Early Middle Triassic trace fossils from the Luoping Biota, southwest**  
2 **China: evidence of recovery from mass extinction**

3  
4 Mao Luo<sup>a, b, c, \*</sup>, G. R. Shi<sup>a</sup>, Shixue Hu<sup>d</sup>, Michael J. Benton<sup>e</sup>, Zhong-Qiang Chen<sup>b, \*\*</sup>, Jinyuan  
5 Huang<sup>d</sup>, Qiyue Zhang<sup>d</sup>, Changyong Zhou<sup>d</sup>, Wen Wen<sup>d</sup>

6  
7 <sup>a</sup>*Deakin University, Geelong, Australia. School of Life and Environmental Sciences & Centre*  
8 *for Integrative Ecology, (Burwood Campus). 221 Burwood Highway, Burwood Victoria, 3125*

9  
10 <sup>b</sup>*State Key Laboratory of Biogeology and Environmental Geology, China University of*  
11 *Geosciences, Wuhan 430074, China*

12  
13 <sup>c</sup>*State Key Laboratory of Geological Processes and Mineral Resources, China University of*  
14 *Geosciences, Wuhan 430074, China*

15  
16 <sup>d</sup>*Chengdu Centre of China Geological Survey, Chengdu 610081, China*

17  
18 <sup>e</sup>*School of Earth Sciences, University of Bristol, Bristol, BS8 1RJ, UK*

19  
20 \*\*Email address: [m.luo@deakin.edu.au](mailto:m.luo@deakin.edu.au) (M. Luo), [zhong.qiang.chen@cug.edu.cn](mailto:zhong.qiang.chen@cug.edu.cn) (Z.Q. Chen)

21  
22  
23 **Abstract**

24  
25  
26 Trace fossils have proven useful for studying the timing and process of biotic recovery  
27 after the Permian–Triassic Mass Extinction (PTME). Recovery stages are defined by  
28 comparing successive ichnoassemblages from the latest Permian to the early Middle Triassic.  
29 Lower Triassic trace fossils have been explored in some detail, but those of the lower Middle  
30 Triassic are less well known. Here, well-preserved fossil materials from the Luoping Biota  
31 from Yunnan Province, South China suggest that a fully recovered shallow marine ecosystem  
32 was re-established by the early Middle Triassic. Trace fossil assemblages of the Luoping  
33 Biota are characterized by high ichnodiversity, with 14 ichnogenera in the shallow marine

34 environment of an intra-carbonate platform basin, and nine ichnogenera in the subtidal  
35 environment. Such moderate to high ichnodiversity, together with a marked increase in  
36 burrow sizes and the common occurrence of key ichnotaxa (e.g. *Rhizocorallium* and  
37 *Thalassinoides*) suggest that the ichnofauna had reached recovery stage four. In contrast, non  
38 turbiditic strata of the offshore setting record only three ichnogenera, with bioturbation  
39 indices never exceeding one. Periodic anoxia in bottom waters was presumably the main  
40 control for such a protracted trace fossil recovery in an offshore setting, which otherwise  
41 aided the fine preservation of body fossils of the Luoping Biota. Furthermore, event  
42 sedimentation (turbidite deposits) in the offshore setting incorporates moderate ichnodiversity  
43 and moderate to high bioturbation indices, both interpreted as a result of short-term  
44 colonization by transported infaunal animals from proximal settings. The occurrence of  
45 variable crustacean traces (e.g. *Sinusichnus*, *Spongiomorpha*, and *Thalassinoides*) at  
46 Luoping and the locomotion traces of marine reptiles, together with abundant fishes and fossil  
47 decapods, highlights the value of trace fossils in ecosystem reconstruction after the PTME.

48

49 Keywords: biotic recovery, ichnological parameter, Guanling Formation, Yunnan, South  
50 China

51

52

53

## 54 **1. Introduction**

55

56 The Permian–Triassic Mass Extinction (PTME), with approximately 90% loss of marine  
57 invertebrate and ~ 80% of terrestrial vertebrate species, is considered the most severe in its  
58 ecological impact on both marine and continental ecosystems (Erwin et al., 2002; Erwin,  
59 2006; McGhee et al., 2004). It was not until the early Middle Triassic that fully recovered  
60 shallow marine ecosystems were re-established (Chen and Benton, 2012). The PTME and  
61 subsequent recovery have been widely studied, with key questions regarding the extinction  
62 mechanism and recovery process remaining open for continued research (Chen and Benton,  
63 2012; Foster and Twitchett, 2014).

64 Trace fossils have proven useful as a means of deciphering the timing and patterns of  
65 biotic recovery after the PTME (Twitchett and Wignall, 1996; Pruss and Bottjer, 2004;  
66 Twitchett, 2006; Chen et al., 2011, 2012; Hull and Darroch, 2013). Trace fossils provide  
67 invaluable information regarding biotic perturbations that is not readily available through

68 geochemical, sedimentological, and modelling-based studies (Morrow and Hasiotis, 2007;  
69 Zonneveld, 2011). Trace fossils represent the activities of both skeletonized and soft-bodied  
70 organisms. Soft-bodied organisms account for a large percentage of the total biomass within  
71 marine ecosystems (Allison and Briggs, 1991; Sperling, 2013), but are typically only  
72 preserved in the form of trace fossils. Hence, ichnofossils potentially provide more complete  
73 records of the behaviours of both infaunal and epifaunal organisms than do body fossils, thus  
74 facilitating the study of community structures and composition (Morrow and Hasiotis, 2007).

75 Lower Triassic trace fossils from all over the world have been studied extensively,  
76 yielding key data on the timing and process of recovery of trace-making organisms from the  
77 PTME (e.g. Twitchett and Wignall, 1996; Twitchett, 1999; Pruss and Bottjer, 2004; Twitchett  
78 and Barras, 2004; Beatty et al., 2008; Fraiser and Bottjer, 2009; Chen et al., 2011; 2012, 2015;  
79 Zonneveld et al., 2010; Knaust, 2010; Hofmann et al., 2011; 2015; Luo, 2014; Luo and Chen,  
80 2014; Shi et al., 2015; Baucon and Carvalho, 2016; Luo et al., 2016; Feng et al., 2017a, b).  
81 Recovery stages were defined by comparing ichnological parameters of locally studied  
82 ichnoassemblages from the Early Triassic with those from the latest Permian and early Middle  
83 Triassic (e.g. Twitchett and Barras, 2004; Twitchett, 2006; Zonneveld et al., 2010; Pietsch and  
84 Bottjer, 2014). These comparisons suggest a step-wise recovery of trace-making organisms, as  
85 documented by the gradual increase in ichnodiversity, burrow size, tiering level, and the  
86 appearance of key ichnotaxa, from the Griesbachian to Spathian (Twitchett, 2006; Pietsch and  
87 Bottjer, 2014). Meanwhile, highly diverse ichnoassemblages discovered in the earliest  
88 Triassic suggest the presence of refugia in certain high-latitude regions and some potential  
89 equatorial regions, which facilitated a faster recovery of trace makers (e.g. Zonneveld et al.,  
90 2010; Knaust, 2010; Godbold et al., 2017).

91 Despite these intensive ichnological studies of Lower Triassic successions around the  
92 world, relatively little attention has been paid to trace fossils from the pre- and post-recovery  
93 intervals (Wignall et al., 1995, 1998; Zonneveld et al., 2001; Zhao et al., 2010; Ding et al.,  
94 2016; Uchman et al., 2016; Feng et al., 2017c), in order to better understand the timing and  
95 pattern of biotic recovery.

96 Recently, the lower Middle Triassic Guanling Formation from Luoping County in Yunnan  
97 province, Southwestern China has attracted substantial attention for the discovery of the  
98 Luoping Biota (Zhang et al., 2008a; 2009; Hu et al., 2011; Chen and Benton, 2012; Feldmann  
99 et al., 2012, 2015; Wen et al., 2012, 2013; Benton et al., 2013; Huang et al., 2013; Liu et al.,  
100 2014; Schweitzer et al., 2014; Zhang et al., 2014). Prolific vertebrate and invertebrate fossils  
101 from this biota record a well-developed shallow marine ecosystem in the middle-late Anisian,

102 suggested as marking the final stage of recovery after the PTME (Hu et al., 2011; Chen and  
103 Benton, 2012; Benton et al., 2013; Liu et al., 2014). Meanwhile, trace fossils (including  
104 coprolites) are similarly well preserved in association with body fossils in the Luoping Biota.  
105 They provide an extraordinary window into the behaviours of trace-making organisms from a  
106 stabilized, fully recovered shallow marine ecosystem after the PTME. Although some  
107 exceptionally preserved examples of coprolites and paddle imprints of nothosaurs from the  
108 Luoping Biota sites have been recently studied (Hu et al., 2011; Zhang et al., 2014; Luo et al.,  
109 2017), most of the burrowing traces remain unstudied.

110 Accordingly, this paper aims to document this trace fossil assemblage from the Luoping  
111 Biota, and compare it with those from Lower Triassic successions of South China and other  
112 regions of the world. The possibility of using the Luoping trace fossil records as a template to  
113 interpret the timing of recovery of trace-making organisms is also explored.

114

## 115 **2. Geological setting, stratigraphy and depositional environment**

116

### 117 *2.1. Geological setting and stratigraphy*

118

119 The three studied sections are located in Luoping County, eastern Yunnan Province,  
120 Southwest China (Fig. 1). During the early Middle Triassic, Luoping, together with its border  
121 areas between eastern Yunnan and western Guizhou Provinces, was located on the  
122 southwestern part of the Yangtze Platform and separated from the Nanpanjiang Basin by a  
123 shoal complex (Feng et al., 1997; Lehrmann et al., 2005; Enos et al., 2006; Fig. 1B). Within  
124 the vast Yangtze Platform interior, several spatially and temporally separated intraplatform  
125 basins or depressions with exceptional fossil preservation, namely the Panxian, Luoping,  
126 Xingyi, and Guanling, have been recognized from the late Anisian, late Ladinian and Carnian  
127 intervals, respectively (Hu et al., 2011; Benton et al., 2013). These basins shared similar  
128 features, including restricted circulation, density stratification of the water column, and  
129 dysoxic to anoxic bottom waters during the burial of these exceptionally preserved vertebrate  
130 faunas through various stages of the Triassic (Benton et al., 2013). At Luoping, abundant  
131 marine reptile faunas were preserved in a basinal setting represented by the upper part of  
132 Member II of the Guanling Formation (Hu et al., 2011). The highly fossiliferous, dark micritic  
133 limestone of the upper part of Member II can be traced over an area of around 200 km<sup>2</sup>  
134 (Benton et al., 2013). Member I and the lower–middle parts of Member II of the Guanling

135 Formation record similar successions over the entire Yangtze Platform interior region in the  
136 Yunnan-Guizhou border areas (Enos et al., 2006; Feng et al., 2017b, 2017c).

137 The Guanling Formation is subdivided into two members. Member I is dominated by  
138 siliciclastic sediments representing deposition in subtidal to intertidal environments (Hu et al.,  
139 1996), whereas Member II comprises micritic limestone, bioclastic limestone, oncoidal  
140 limestone and dolomite in the lower and middle parts, and black muddy limestone, cherty  
141 limestone, and grey dolomite in the upper part. Integration of sedimentary facies analysis,  
142 palaeontology and taphonomy indicates that the lower and middle parts of Member II were  
143 deposited in relatively open, shallow marine settings, whereas the upper portion of the  
144 member was deposited in a low-energy, semi-enclosed intraplateau basin influenced by  
145 episodic storms (Hu et al., 2011). The Guanling Formation in the Luoping area, overall,  
146 records a progressively deepening succession (Zhang et al., 2008a).

147 The *Nicoraella kockeli* Conodont Zone has been detected in the upper part of Member II.  
148 This conodont zone includes elements, such as *Nicoraella germanicus*, *Nicoraella kockeli* and  
149 *Cratognathodus* sp., indicative of the Pelsonian age of the middle Anisian (Zhang et al.,  
150 2009). The underlying Member I of the Guanling Formation yields the bivalves *Myophoria*  
151 (*Costatoria*) *goldfussi mansuyi* Hsü, *Unionites spicatus* Chen, *Posidonia* cf. *pannonica* Moj,  
152 and *Natiria costata* (Münster), and contains several clay beds. This bivalve assemblage is of  
153 early Anisian age in South China (Zhang et al., 2008a), and the clay beds have been regarded  
154 as correlation markers for the base of the Anisian in southwest China (Enos et al., 2006;  
155 Zhang et al., 2009).

156

157

## 158 2.2. Interpretation of depositional environment

159

160

161 Three sections have been excavated systematically at Luoping for fossil collection and  
162 study of the stratigraphy and depositional environment. They are named Dawazi (or Daaози)  
163 (DWZ), Shangshikan (SSK), and Xiangdongpo (XDP), respectively (Zhang et al., 2008a;  
164 2009; Huang et al., 2009; Bai et al., 2011; Hu et al., 2011; Figs. 1A, 2). The Middle Triassic  
165 successions in these three excavation sites correlate well with each other by a sharply based,  
166 bioturbated wackestone separating the upper and lower fossiliferous units (Bai et al., 2011;  
167 Zhang et al., 2014). Further, the three sections are located close together, and individual  
168 limestone marker beds can be traced across country between the sections. The thickly bedded

169 limestone unit bears extremely consistent features, including thorough bioturbation, the  
170 inclusion of burrows filled by silica concretions, and almost uniform thickness, thus serving  
171 as a clear marker unit. Following this recognition, three stratigraphic units have been defined  
172 and correlated in the three sections. The documented sedimentary features of these units and  
173 their environmental interpretations are as below.

174

#### 175 *2.2.1. Unit A (shallow to deep subtidal)*

176

177 Unit A is composed of medium-to thick-bedded bioclastic wackestone and oncoidal  
178 pack-wackestone with a small proportion of calcareous mudstone (Fig. 3A, G, H). In DWZ  
179 and SSK, stromatolitic bindstones also occur as major constituents. Fragmented bivalve shells,  
180 echinoderms, and ostracods are the main skeletal components in wackestone and packstone,  
181 with faecal pellets as subordinate grain types. Planar lamination is well developed in both  
182 wackestone and carbonate mudstone facies, with bioturbation index (BI) ranging from 1 to 4  
183 (BI schemes follow Reineck, 1963, and Taylor and Goldring, 1993). BI 1 represents sparse  
184 disruption of sediments (1–4%) whereas BI 4 is characterized by intense bioturbation  
185 (61–90%). Wavy crinkled lamination developed locally in the dolomitic limestone (Fig. 3H)

186 The dominance of muddy facies in this association indicates a deep subtidal setting.

187 Oncoids indicate moderate energy conditions in shallow water. Stromatolitic build-ups have  
188 been observed from shallow to deep subtidal environments in the Triassic (e.g. Flügel et al.,  
189 2004, p. 57; Ezaki et al., 2008, 2012). Thus, a shallow to deep subtidal setting is interpreted  
190 for Unit A.

191

#### 192 *2.2.2. Unit B (offshore)*

193

194 Unit B is composed mainly of very thin bedded (1–3 cm) marly carbonate mudstones  
195 intercalated with very thin-bedded (1 cm) black shales (Fig. 3B–C), bioturbated wackestones,  
196 and minor thin-bedded packstones. Thin bedded to lenticular chert layers and cherty nodules  
197 are also prominent. Planar lamination and reticulated ridge structures (Fig. 3B–C; Luo et al.,  
198 2013) are pervasively developed in marly carbonate mudstones, followed by locally occurring  
199 convolute lamination. Disseminated pyrite crystals and pyrite framboids are common in marly  
200 carbonate mudstones (Fig. 8A, C), in which bioturbation is absent except for a few surficial  
201 trails preserved on bedding planes. Locally, normally graded packstone beds have a basal  
202 sharp and erosive contact, which are overlain by planar to convolute lamination and massive

203 carbonate mudstones (Fig. 3D). These coarse-grained beds are also characterized by pervasive  
204 bioturbation. Thick-bedded, sharp-based nodular (bioturbated) wackestone marker layers  
205 separate the upper and lower marly carbonate mudstone beds/units (Fig. 3E), in which  
206 abundant well-preserved vertebrate and invertebrate fossils have been discovered, respectively  
207 (Fig. 2; Bai et al., 2011; Benton et al., 2013; Zhang et al., 2014; Luo et al., 2017). Several ash  
208 layers also occur intercalated in the marly carbonate mudstones of Unit B (Fig. 2).

209 The overall fine-grained sediments of Unit B are interpreted as deposits from suspension in  
210 a low-energy environment with weak current activity. This is shown by the thinly laminated  
211 nature of the marly carbonate mudstones and shales. Reticulated ridge structures have been  
212 interpreted as indications of benthic microbial mats (Luo et al., 2013). The wide occurrence of  
213 benthic microbial mats required a water depth within the photic zone, the lower limit of which  
214 is 80–100 m (e.g. James and Bourque, 1992, p. 326). The packstone beds, with their overlain  
215 planar/convolute-laminated sediments and massive carbonate mudstones represent Ta, Tb and  
216 Te of the Bouma Sequence, which are interpreted to be the result of low-density, dilute  
217 turbiditic currents (e.g. Walker, 1992). Similar thin-bedded turbidite deposits have also been  
218 observed in the Meride Limestone of the Monte San Giorgio Lagerstätte (Stockar, 2010).  
219 Furthermore, turbidite current activity is further supported by the bedded nature of the chert  
220 beds, which is interpreted as the result of rapid, turbiditic input of biogenic sediments (e.g.  
221 McBride and Folk, 1979; Bustillo and Ruiz-Ortiz, 1987). The common occurrence of pyrite  
222 framboids in the carbonate mudstones possibly indicates anoxic bottom water conditions. To  
223 sum up, Unit B represents deposition in an anoxic offshore environment.

224

### 225 *2.2.3. Unit C (offshore transition)*

226

227 Unit C is composed of thin- to medium-bedded hummocky cross-stratified wackestones  
228 (Fig. 3F), carbonate mudstones, with minor intraclastic floatstones and bioclastic packstones.  
229 Wackestone beds are sharply to erosively based, with a few cherty nodules present locally.  
230 Convolute lamination and gutter casts also occur. Bioturbation is pervasive in the  
231 wackestones and carbonate mudstones. Intraclasts are composed of carbonate mudstone.  
232 Packstone layers are lenticular and have graded bedding in the basal parts.

233 Packstones with a graded basal part, together with their lenticular morphology are most  
234 likely associated with storms. Such storm activity is also indicated by the frequent occurrence  
235 of hummocky cross-stratification, which is interpreted as a combination of waning oscillatory  
236 flow and unidirectional currents created by periodic storm events (Dott and Bourgeois, 1982;



237 Dumas and Arnott, 2006). Thus, Unit C is interpreted as the deposits of an offshore  
238 transitional environment.

239

240

### 241 **3. Ichnological features of the Luoping Biota**

242

243 Fourteen ichnotaxa have been identified from the three studied sections through Member II  
244 of the Guanling Formation. These ichnotaxa are distributed in both the lower and upper fossil  
245 layers and strata above and below (Fig. 2). Detailed descriptions of all discovered trace fossils  
246 and ichnological parameters are presented below.

247

#### 248 *3.1. Ichnological descriptions*

249

##### 250 *3.1. Archaeonassa Fenton and Fenton, 1937*

251

##### 252 *3.1.1. Archaeonassa fossulata Fenton and Fenton, 1937 (Fig. 4A)*

253 Preserved as concave epirelief on upper bedding plane of carbonate mudstone. Grooved  
254 trails are gently curved, and are flanked by rounded ridges. Width of trail is about 10 mm and  
255 length up to 230 mm. Width remains consistent in individual trails.

256

257 *Remarks:* The grooved trail flanked on both sides by rounded ridges is diagnostic of  
258 *Archaeonassa* (Fig. 4A). Although the observed specimen from the DWZ section is similar to  
259 *Helminthopsis*, the meandering characteristics of *Helminthopsis* are more complicated than  
260 those of *Archaeonassa*. *Archaeonassa* is typically preserved in intertidal regimes where such  
261 traces may be abundant (Fenton and Fenton, 1937), and it may also occur more rarely in  
262 shallow marine environments. *Archaeonassa* is also known from continental environments  
263 (e.g. Buckman, 1994; Buatois and Mángano, 2002). *Archaeonassa* can be produced by  
264 various invertebrates, including molluscs and arthropods (Buckman, 1994; Yochelson and  
265 Fedonkin, 1997).

266

##### 267 *3.2. Arenicolites Salter, 1857*

268

##### 269 *3.2.1. Arenicolites isp. (Fig. 4B)*

270 Preserved as paired tubes on upper bedding planes of carbonate mudstones and  
271 wackestones. Tubes are preserved as hollow, funnel-shaped openings with no burrow fill or  
272 probably eroded away. Tube diameters range from 7 to 18 mm and the distance between the  
273 tubes (width) is up to 62 mm. Diameters of the two tubes in a pair are slightly different.

274 *Remarks:* *Arenicolites* and *Skolithos* are difficult to distinguish when they occur densely on  
275 bedding planes. The tube structures are usually paired, justifying a reasonable assignment to  
276 *Arenicolites*. No spreiten structures have ever been observed between the paired tubes,  
277 excluding their assignment to *Diplocraterion*. *Arenicolites* is regarded as an element of the  
278 shallow marine *Skolithos* ichnofacies and firmground *Glossifungites* ichnofacies (e.g. Buatois  
279 and Mángano et al., 2011a; MacEachern et al., 2012), although such biogenic structures also  
280 occur in freshwater deposits (Bromley and Asgaard, 1979). Trace producers include various  
281 worm-like organisms, such as polychaetes (Bradshaw, 2010).

282

### 283 3.3. *Dikoposichnus* Zhang et al., 2014

284

#### 285 3.3.1. *Dikoposichnus luopingensis* Zhang et al., 2014 (Fig. 4C)

286 Large, narrow V-shaped slot-like depressions preserved as single or paired imprints on  
287 both upper bedding plane (concave epireliefs) and sole surfaces (convex hyporeliefs).  
288 Individual imprint is elliptical to sigmoidal, with an anterior sweep at the medial edge. Paired  
289 imprints commonly consist of long (up to 18.7 m) trackways that are 30–70 cm wide.

290

291 *Remarks:* This new trace was introduced by Zhang et al. (2014) based on materials from  
292 bed 107 of the DWZ section. The well-preserved footprints in long trackways are paired,  
293 suggesting the limbs moved in concert. They were interpreted as the paddle imprints of a  
294 limbed vertebrate (e.g. nothosaur) moving in a steady manner over the seabed searching for  
295 prey (Zhang et al., 2014). It is considered to represent the first locomotion record of marine  
296 reptiles from the Mesozoic.

297

### 298 3.4. *Diplocraterion* Torell, 1870

299

#### 300 3.4.1. *Diplocraterion* isp. (Fig. 4D–F)

301 Paired tubes with variable size ranges in both burrow width and diameter. Maximum  
302 burrow diameter can reach 17.5 mm and width of up to 84 mm. There are very delicately

303 preserved spreiten structures within shafts connecting the two tubes. Burrow fill of tubes and  
304 connected shafts have a darker colour than the host rock.

305

306 *Remarks:* In plan view, the dumbbell-shaped structure, in which the paired tubes are  
307 linked by spreiten, justifies assignment to *Diplocraterion*. There is no further evidence of  
308 detailed structures in vertical profiles, which prevents assignment to an ichnospecies. Features  
309 of the spreiten that connect the paired tubes suggest it is protrusive, indicating a downward  
310 movement of trace makers in response to possible erosion of the sediment surface (Bromley,  
311 1996; Buatois and Mángano, 2011a). Dense preservation of these burrows as patch  
312 assemblages indicates some possible opportunistic strategies of the trace makers (e.g. Vossler  
313 and Pemberton, 1988). In particular, variably sized *Diplocraterion* occurring together could  
314 be the product of different generations of animals. *Diplocraterion* is regarded as a dwelling  
315 trace of suspension feeders and has a stratigraphic range from Cambrian to present (Abbassi,  
316 2007). It is a characteristic member of the *Skolithos* ichnofacies, and also the substrate-  
317 controlled *Glossifungites* ichnofacies (MacEachern et al., 2007; Buatois and Mángano,  
318 2011a). It has also been utilized for defining sequence boundaries and stratigraphic correlation  
319 (Taylor and Gawthorpe, 1993; Olóriz and Rodríguez-Tovar, 2000).

320

### 321 3.5. Megagraption *Książkiewicz, 1968*

322

#### 323 3.5.1. Megagraption *irregulare Książkiewicz, 1968 (Fig. 4G)*

324 Cord-sized strings preserved as convex hyporeliefs; burrows meander irregularly and  
325 branching at right angles. Meandering burrows also form irregular, rectangular meshes that  
326 are not closed.

327

328 *Remarks:* The specimen observed at Luoping has diagnostic features including  
329 perpendicular branching angles and unclosed meshes resembling *Megagraption irregulare*.  
330 *Megagraption* is a typical ichnotaxon of flysch strata, usually preserved on sole surfaces in  
331 association with other graphoglyptids. It bears some characteristics resembling  
332 *Protopaleodictyon* (Książkiewicz, 1977; Uchman, 1998). *Megagraption* has been commonly  
333 observed in Permian to Cretaceous flysch strata in China (e.g. Zhang et al., 2008b).

334

### 335 3.6. Palaeophycus *Hall, 1847*

336

337 3.6.1. *Palaeophycus* isp. (Fig. 5A)

338 Simple, horizontal to inclined cylindrical burrows preserved in carbonate mudstones.  
339 Burrows are straight to slightly curved, sub-circular in cross-section. The burrow wall is  
340 smooth, and burrow width ranges from 8 to 13 mm. Burrow linings are typical. Burrow fill is  
341 the same in colour and composition as the host rock.

342

343 *Remarks:* The similarity of the burrow fill and the surrounding host rock and burrow  
344 lining are typical of the ichnogenus *Palaeophycus* (e.g. Osgood, 1970; Pemberton and Frey,  
345 1982). *Palaeophycus* is a facies-crossing ichnogenus and occurs from the Precambrian to  
346 present (Pemberton and Frey, 1982).

347

348 3.7. *Planolites Nicholson, 1873*

349

350 3.7.1. *Planolites* isp. (Fig. 5B)

351 Horizontal, smooth trails that are straight to gently curved. They are circular to elliptical  
352 in transverse section. Burrows are unbranched, and commonly cross-cut each other. Burrow  
353 fill is structureless, and is darker than the host rock. Burrow diameters range from 2.1 to 25.1  
354 mm, and average 10.5 mm.

355

356 *Remarks:* The unlined burrow and its darker colour in contrast to the host rock is  
357 diagnostic of *Planolites*. It is a facies-crossing ichnotaxon, ranging through a wide variety of  
358 environments from shallow to deep marine and also nonmarine. Its producer includes certain  
359 vermiform deposit feeders (e.g. Pemberton and Frey, 1982; Uchman, 1995). *Planolites* also  
360 has a wide stratigraphic range from the Precambrian to present (Häntzschel, 1975).

361

362 3.8. *Rhizocorallium Zenker, 1836*

363

364 3.8.1. *Rhizocorallium* isp. (Fig. 5C)

365

366 Gently inclined to horizontal, U-shaped tubes are preserved as full reliefs in carbonate  
367 mudstones/wackestones. U-tube has dark burrow fill in contrast to the host rock (Fig. 5C). No  
368 spreiten structures are evident between limbed tubes. Burrow size (width of U tube) ranges  
369 from 16 to 43 mm, with an average value of 26.1 mm (Fig. 7C). Clustered individuals cross

370 cut-each. They are also found to cross-cut the previously formed, meshwork burrowing  
371 systems resembling *Thalassinoides*.

372

373 *Remarks:* Specimens from the Guanling Formation in the Luoping area bear certain  
374 characteristics resembling *Rhizocorallium commune* (Knaust, 2013). These include their  
375 gregarious nature, the relatively smaller size compared with *R. jenense* (see below), and their  
376 cross-cutting relationships. However, the absence of scratches along marginal tubes prevents  
377 unequivocal assignment. *Rhizocorallium* can be produced by various animals including  
378 decapods, crustaceans, annelids, polychaetes, and also mayflies (Knaust, 2013).

379

### 380 3.8.2. *Rhizocorallium jenense* Zenker, 1836 (Fig. 5D–F)

381 These U-shaped burrows are isolated, and preserved as horizontal epirelief or hyporeliefs.  
382 Burrow fill has similar colour to the host rock. Typical spreiten structures between the limbed  
383 tubes are characteristic (Fig. 5D–E). The whole U-shaped tubes form long tongue-shaped  
384 structures and even complex spiral burrowing systems. Ornamented faecal pellets are evident  
385 in limbed burrows (Fig. 5F). Burrow width of U-tubes ranges from 27 to 74.5 mm, and  
386 averages 51.3 mm (Fig. 7B).

387 *Remarks:* These specimens are assignable to *Rhizocorallium jenense*, which is  
388 characterized by an elongate morphology, larger size and prominent faecal pellets in limbed  
389 tubes. *Rhizocorallium* is an element of the *Cruziana* ichnofacies and also a representative  
390 ichnotaxon of the firmground *Glossifungites* ichnofacies (Buatois and Mángano, 2011a).  
391 *Rhizocorallium* has been widely recognized in strata from the lower Cambrian to Cenozoic  
392 (e.g. Knaust, 2013). The potential producer of *R. jenense* could be a polychaete (Knaust,  
393 2013).

394

## 395 3.9. *Sinusichnus* Gibert, 1996

396

### 397 3.9.1. *Sinusichnus* isp. (Fig. 5G–H)

398 This trace is preserved as positive or negative hyporeliefs, and can be found over areas  
399 spanning several square decimetres. Horizontal burrows are knobby, and show regular  
400 sinuous tunnels, but less regular to straight tunnels are also evident/present in the same  
401 branching system (Fig. 5G). Branching points usually comprise three points forming a Y- or  
402 T-shaped junction (Fig. 5G). In some cases, two closely emplaced triple junctions form an H-  
403 like configuration. Four-pointed branching is also apparent locally. The burrow system

404 penetrates into the sediment at very shallow depths (no more than 1.5 cm). Retrusive spreiten  
405 were not observed. Diameters of sinuous burrows remain identical in each distinct burrow  
406 system, but vary slightly between different specimens. Measurements of 102 specimens reveal  
407 a burrow width ranging from 4 to 16 mm, with an average value of 8.8 mm.

408  
409 *Remarks:* The newly discovered traces are extremely similar to the ichnogenus  
410 *Sinusichnus* established by Gibert (1996). This is revealed by the regular sinuous and  
411 branching morphology of the horizontal tunnels. In addition, the significant relationship  
412 between wavelength ( $\lambda$ ) and amplitude (A) in the Luoping specimens has also been found in  
413 typical *S.sinuosus* (Gibert et al., 1999a). Apart from the type ichnospecies *S. sinuosus*  
414 established by Gibert (1996), Kapper (2003) proposed another ichnospecies, *S. priesti*, based  
415 on specimens from Upper Cretaceous strata in Germany. The only feature distinguishing *S.*  
416 *sinuosus* from *S. priesti* is the presence of bioglyphs in the latter. No scratch marks or  
417 bioglyphs are evident on the branching burrows observed herein. In addition, the knobby  
418 appearance of the specimen suggests some lining of the burrows, a feature that is not present  
419 in *Sinusichnus*. It is noted also that the specimens studied here are less regular in some parts  
420 of the burrow segments compared with those from Pliocene and Miocene strata (e.g. Buatois  
421 et al., 2009; Belaüstegui et al., 2014). These features make it difficult to assign the specimen  
422 to any of the ichnospecies established. The trace *Sinusichnus* can be produced by decapod  
423 crustaceans and isopods, and has a stratigraphical range from Middle Triassic to Pliocene (e.g.  
424 Gibert, 1996; Buatois et al., 2009; Belaüstegui et al., 2014; Knaust et al., 2016).

425  
426 *3.10. Spongeliomorpha Saporta 1887*

427  
428 *3.10.1. Spongeliomorpha isp. (Fig. 6A)*

429 This trace is preserved as full relief on the upper surface of carbonate mudstones. Burrows  
430 exhibit Y-shaped branching, with delicate, longitudinal scratch marks seen on burrow wall  
431 surface. There is enlargement at burrow intersection. Burrow diameter ranges from 21 to 27  
432 mm.

433  
434 *Remarks:* The observed specimens bear characteristics, such as Y-shaped branching and  
435 scratched burrow walls, typical of *Spongeliomorpha*. However, it should be noted that the  
436 longitudinal striae (scratch marks) are different from the transversely oriented striations

437 reported in some previous work (e.g. Bromley and Asgaard, 1979), nor are they comparable  
438 with those observed in *S. iberica* (e.g. Melchor et al., 2009). An assignment at ichnospecies  
439 level is unresolved. Although several animals have been proposed as the possible trace makers  
440 of *Spongiomorpha*, the enlargement at the bifurcating junction, together with scratch marks  
441 on the burrow wall surface, indicate that a decapod is most likely the trace maker for  
442 *Spongiomorpha* isp. at Luoping. This trace has been found in both marine and nonmarine  
443 environments, and has a stratigraphical range from Early Permian to Miocene (Bromley and  
444 Asgaard, 1979; Carmona et al., 2004; Melchor et al., 2009).

445

446

### 447 3.11. *Taenidium* Heer 1877

448

#### 449 3.11.1. *Taenidium barretti* Bradshaw, 1981 (Fig. 6B)

450 Unlined cylindrical burrow preserved in carbonate wackestone. In vertical profile,  
451 sinuous burrows contain dark, articulated burrow fill alternating with light meniscate partings.  
452 The alternating two types of sediment have varying thickness and are unevenly spaced.  
453 Burrow is unbranched, and has a consistent diameter of 10 mm.

454

455 *Remarks:* The specimen has a striking resemblance to *Beaconites antarcticus* as  
456 illustrated by Graham and Pollard (1982). However, following the reclassification of  
457 *Beaconites*, *Taenidium* and *Ancorichnus* (Keighley and Pickerill, 1994), this trace fossil  
458 should be renamed as *Taenidium barretti*. The taxonomy of meniscate burrows was  
459 comprehensively reviewed and revised by D'Alessandro and Bromley (1987). Three  
460 ichnospecies were proposed as valid for *Taenidium* before *Taenidium barretti*, namely *T.*  
461 *serpentinum*, *T. cameronensis*, and *T. satanassi* (D'Alessandro and Bromley, 1987). The  
462 unbranched, meniscate structures observed herein have very gentle curvature, and consist of  
463 unevenly distributed dark and light menisci that are deeply arcuate and tightly packed. These  
464 features justify assignment to *Taenidium barretti*. *Taenidium* has been reported from strata  
465 ranging from the Cambrian to Eocene (D'Alessandro et al., 1986; D'Alessandro and Bromley,  
466 1987; Yang et al., 2004), but most occurrences are from the Silurian–Devonian, and the  
467 Cretaceous to Eocene (e.g. Häntzschel, 1975, p.W84; Bradshaw, 1981).

468

469

### 470 3.12. *Thalassinoides* Ehrenberg, 1944

471

472 3.12.1. *Thalassinoides suevicus Rieth, 1932 (Fig. 6C)*

473 The burrows are preserved as either concave epirelief or convex hyporelief on carbonate  
474 mudstones/wackestones. Burrows typically occur as Y-shaped branching systems and have  
475 swollen bumps at conjunction points (Fig. 6C). Burrow surface is smooth. Burrow sizes range  
476 from 5 to 30 mm, and average 17.9 mm. Burrow shafts usually form complicated meshworks  
477 covering a maximum area of up to tens of square metres. Burrow penetration depth is shallow  
478 (no more than 5 cm). On some horizons of the XDP section, larger Y-shaped burrows systems  
479 were cross-cut by U-shaped *Rhizocorallium* isp.

480

481 *Remarks:* This trace is characterized by its Y-shaped branching. The swollen part at the  
482 junctions implies that these *Thalassinoides* traces were produced by decapod crustaceans  
483 (Bromley and Frey, 1974; Carmona et al., 2004; Carvalho et al., 2007). Such a trace fossil is  
484 usually interpreted as a dwelling or feeding structure produced by detritus-feeding crustaceans  
485 in shallow to deep marine environments (Myrow, 1995; Carvalho et al., 2007). Besides,  
486 *Thalassinoides* burrows are also present in the firmground substrate of the *Glossifungites*  
487 ichnofacies immediately after the end-Permian crisis (Chen et al., 2015). *Thalassinoides* has a  
488 stratigraphical range from Cambrian to present (Myrow, 1995), but a decapod origin of such  
489 traces has been suggested for Devonian examples (e.g. Carmona et al., 2004).

490

491 3.13. *Undichna Anderson, 1976*

492

493 3.13.1. *Undichna unisulca Gibert et al., 1999 (Fig. 6D)*

494 These are unpaired sinuous ridges on sole surfaces of bedding planes of  
495 wackestones/packstones. Two single trails were identified, which are preserved as regular  
496 sinusoidal strings with equal wavelength and amplitude. The sinuous trail is composed of two  
497 to three ridges separated by subtle grooves.

498

499 *Remarks:* The Luoping specimens of single-waved trails are extremely similar to  
500 *Undichna unisulca* diagnosed by Gibert et al. (1999b) and Morrissey et al. (2004) in both  
501 morphology and preservation, and thus justify assignment to this ichnospecies. This trace has  
502 been interpreted to be generated by a fish swimming with its caudal fin in contact with the  
503 substrate (Gibert et al, 1999b). As fishes diversified from the Ordovician onwards, their  
504 behavioural product, *Undichna* also has a very wide stratigraphic distribution in the



505 Palaeozoic, Mesozoic and Cenozoic (Gibert et al., 1999b., Gibert, 2001; Benner et al., 2009;  
506 Fillmore et al., 2011).

507

508

509 *3.14. Zoophycos Massalongo, 1855*

510

511 *3.1.14. Zoophycos isp.? (Fig. 6E, F)*

512 These are spiral-shaped structures composed of U-shaped protrusive, primary laminae of  
513 variable orientation. Primary laminae arrange in helicoid spirals to form an overall elliptical  
514 shape, with no marginal tubes observed.

515

516 *Remarks:* The primary laminae forming helicoid spirals is characteristic of *Zoophycos*  
517 (e.g. Uchman, 1995), but the incomplete preservation of the specimen and absence of  
518 marginal tubes prevent assignment to an ichnospecies. The origin of *Zoophycos* is unresolved,  
519 although it is generally assumed to have been made by deposit-feeding organisms (Uchman,  
520 1995; 1998), with sipunculoids, polychaete annelids, and enteropneust hemichordates all  
521 possible trace makers (e.g. Wetzel and Werner, 1981; Ekdale and Lewis, 1991; Kotake, 1992).  
522 *Zoophycos* has a stratigraphic age range from Cambrian to present (e.g. Zhang et al., 2015),  
523 and its trace maker transferred from shallow water environments in the Palaeozoic to deep  
524 marine environments since the Cretaceous (e.g. Seilacher, 1974; Zhang et al., 2015).

525

526

#### 527 **4. Eco-ichnological characteristics**

528

529 *4.1. Abundance and ichnodiversity*

530

531 Fourteen ichnogenera were recorded from the three studied sections at Luoping. Among  
532 these, six ichnogenera are more abundant than the others, and these form dense assemblages  
533 at particular horizons. These are *Arenicolites*, *Dikoposichnus*, *Diplocraterion*, *Planolites*,  
534 *Rhizocorallium*, and *Thalassinoides*. Other traces are only locally developed.

535 The offshore setting of Unit B is characterized by very low ichnodiversity and low BI. Non-  
536 turbiditic strata, as represented by marly carbonate mudstone and shales are nearly devoid of  
537 bioturbation, with only *Dikoposichnus*, *Megagraption* and *Undichna* preserved as surficial  
538 trails/tracks on bedding planes. It is the same case for both the upper and lower ‘fossil

539 horizons'. The sharply to erosively based turbidite beds, in contrast, have a moderate to high  
540 BI and a moderately diverse ichnoassemblage. Ichnotaxa in those event beds include  
541 *Diplocraterion*, *Planolites*, *Rhizocorallium*, *Sinusichnus*, *Taenidium*, and *Thalassinoides*.  
542 There is a marked increase in BI for the offshore transition of Unit C. Most of the beds were  
543 variously bioturbated, with BI ranging from two to four. However, the ichnodiversity remains  
544 low. Unit A saw the highest level of both BI and ichnodiversity. Nine ichnogenera were  
545 discovered from this unit, including *Archaeonassa*, *Arenicolites*, *Palaeophycus*, *Planolites*,  
546 *Sinusichnus*, *Rhizocorallium*, *Spongeliomorpha*, *Thalassinoides*, and ? *Zoophycos*. BI levels  
547 also increased, from one to four.

548

#### 549 4.2. Burrow size

550

551 Burrow sizes of the abundantly preserved traces of the Luoping Biota were analyzed  
552 statistically. Burrow forms analyzed include *Diplocraterion*, *Planolites*, *Rhizocorallium* and  
553 *Thalassinoides* (Fig. 7A–D).

554 The average burrow width of *Diplocraterion* is 26.4 mm based on measurements of 135  
555 individuals. *Planolites* has a wide range of burrow diameters (2.1–25.1 mm), average 10.5  
556 mm (Fig. 7A). Two ichnospecies of *Rhizocorallium* were measured separately. For the larger  
557 group, burrow width of the U-tubes averages 51.3 mm (Fig. 7B), whereas the average width  
558 for the smaller one is 26.1 mm. For the maze-work of *Thalassinoides*, the burrow widths range  
559 from 5 to 30 mm, with a mean value of 17.9 mm, based on 104 measurements (Fig. 7D).

560

#### 561 4.3. Tiering level and complexity

562

563 Tiering level is practically evaluated by measuring the penetration depth of trace fossils, to  
564 explore ecospace utilization of sediment. Trace fossils are preserved at very shallow depths in  
565 marly carbonate mudstones of Unit B, where trails, such as *Megagraption*, *Undichna* and  
566 *Dikoposichnus*, occupied only the upper 1–2 cm of the sediments. Vertical burrows, such as  
567 *Diplocraterion* and *Arenicolites*, also penetrate to depths of no more than 3 cm. Trace fossils  
568 in Unit C also have very shallow penetration depths. Those complex traces such as  
569 *Rhizocorallium*, *Spongeliomorpha* and *Thalassinoides*, occupied only the surficial 2–4 cm of  
570 the sediments.

571 Turbidite deposits in Unit B, on the other hand, have deeper burrows than their  
572 surrounding non-turbiditic sediments. Vertically oriented *Taenidium* has a penetration depth

573 of 5 cm. The silicified *Thalassinoides* burrows in marked horizons have an even deeper  
574 penetration depth up to 10 cm.

575

576

## 577 **5. Discussion**

578

### 579 *5.1. Decoupled features between trace fossils and body fossils in the Luoping Biota*

580

581 There is decoupling between the preservation of trace fossils and body fossils at Luoping.  
582 In particular, the lower and upper fossiliferous units preserve abundant vertebrate and  
583 invertebrate fossils, but with only a few superficial trace fossils, such as *Dikoposichnus*,  
584 *Megagraption*, and *Undichna*. Such a decoupling effect has long been recognized by  
585 ichnologists, who explain this phenomenon by differential preservational conditions between  
586 trace fossils and body fossils (e.g. Buatois and Mángano, 2011a). Indeed, at Luoping, such  
587 decoupling might have resulted from periodic anoxia in offshore environments, which largely  
588 inhibited colonization by trace makers. The upper and lower fossiliferous units are both  
589 characterized by thin-bedded marly carbonate mudstones intercalated with shales,  
590 representing quiet, offshore depositional environments. The black sediments, and the common  
591 occurrence of dispersed pyrite crystals suggests possible periodic anoxia in offshore  
592 environments. Statistical analysis of the pyrite framboids in carbonate mudstones supports  
593 such a notion. Measurements of pyrite framboids from two strata of the lower fossiliferous  
594 bed/unit of the SSK section reveal mean diameters of 6.60  $\mu\text{m}$  and 5.34  $\mu\text{m}$ , with standard  
595 deviations of 1.21 and 1.77, respectively (Fig. 8A–D). This result indicates an anoxic marine  
596 environment (e.g. Wilkin et al., 1996; Wignall and Newton, 1998).

597 Due to such periodic anoxia in bottom waters, bioturbation was largely inhibited. When  
598 there were transient oxic conditions, fishes, marine reptiles, and a few invertebrates could  
599 survive and leave their traces of activity, represented by the occurrence of *Undichna*,  
600 *Dikoposichnus*, and *Megagraption*. It is noted that the presence of *Undichna* and  
601 *Dikoposichnus*, together with the abundant preservation of fishes and marine reptile fossils in  
602 the Middle Triassic Luoping biota may reflect the déjà vu effect (*sensu* Buatois and Mángano,  
603 2011b).

604 Interestingly, at Luoping, the preservational conditions of the Luoping Biota seem to  
605 have aided the preservation of trace fossils in the lower and upper fossiliferous units.  
606 Specifically, the sealing effect of microbial mats played a significant role in the preservation

607 of both (including coprolites). When the Luoping animals died and settled on the sea floor, the  
608 episodic anoxic environment inhibited rapid decay of the animals. With a further sealing  
609 effect from microbial mats, animal carcasses were rapidly coated by mats and protected from  
610 disarticulation by turbulent currents (e.g. Luo et al., 2013). Such establishment of firmground  
611 substrates might have further stabilized the burrowed sediment surfaces, and enhanced the  
612 preservation of those surficial traces (e.g. Buatois and Mángano, 2013).

613

## 614 5.2. Comparison with Early Triassic trace fossil assemblages

615

616 A four-stage recovery model based on multiple ichnological parameters has been  
617 proposed to summarize the recovery process of trace makers at various stages of the Early  
618 Triassic (e.g. Twitchett, 2006), which was later adopted by several researchers (e.g. Chen et  
619 al., 2011; Hofmann et al., 2011; Luo et al., 2016). Low ichnodiversity, ichnofabric indices,  
620 shallow tiering level and small burrow sizes characterize the early recovery stages (e.g. one to  
621 two). This is the case for most ichnoassemblages from shallow marine environments dating  
622 from Griesbachian to Dienerian (e.g. Chen et al., 2011; Zhao and Tong, 2010; Zhao et al.,  
623 2015). Ichnological parameters show substantial increases in Smithian to Spathian strata from  
624 certain regions of South China, eastern Australia, and Western United States, where the  
625 recovery stage increased to three or four (e.g. Chen et al., 2011; 2012; Mata and Bottjer, 2011;  
626 Luo et al., 2016; Feng et al., 2017). However, not all trace makers had recovered to such an  
627 advanced stage in the Smithian and Spathian, suggesting marked variation in recovery rate,  
628 most likely controlled by the heterogeneous development of oxic facies (Luo et al., 2016).

629 At Luoping, nine ichnogenera were discovered from the subtidal deposits of Unit A. Key  
630 ichnogenera, such as *Rhizocorallium* and *Thalassinoides* are also commonly found. These  
631 observations, together with a moderate to high bioturbation level suggest recovery stage four.  
632 Burrow sizes of several ichnogenera (e.g. *Planolites*, *Rhizocorallium* and *Thalassinoides*) also  
633 show a marked increase compared with their Lower Triassic counterparts. For example,  
634 *Planolites* from subtidal environments at Luoping records a mean diameter of 10.5 mm,  
635 which is equivalent to that from the Upper Permian Bellerophon Formation of Northern Italy,  
636 obviously larger than Lower Triassic *Planolites* from various regions (e.g. Twitchett, 1999;  
637 Pruss and Bottjer, 2004; Zonneveld et al., 2010; Chen et al., 2011; 2012; Luo et al., 2016;  
638 Feng et al., 2017a; Fig. 9A), except the late Spathian *Planolites* from the Yashan section of  
639 South China (Chen et al., 2011). *Rhizocorallium* is rare in the Lower Triassic, with only a few  
640 studies mentioning their burrow sizes. The Induan *Rhizocorallium* from the Montney

641 Formation of Canada has larger burrow widths even compared to late Early Triassic examples  
642 (e.g. Zonneveld et al., 2010; Fig. 9B). This might relate to the presence of refugia in those  
643 areas, which facilitate the survival of trace makers. Burrow widths of *Rhizocorallium* from the  
644 Smithian Sinbad Limestone, and the Spathian Virgin Limestone of the United States are  
645 generally less than 26 mm, with average values of 6 mm and 14 mm respectively (Pruss and  
646 Bottjer, 2004; Fraiser and Bottjer, 2009). An obvious increase in *Rhizocorallium* burrow size  
647 in the Spathian is also revealed by their occurrence in the Spathian Nanlinghu Formation of  
648 the Susong section, South China, and in the Tvillingodden Formation of western Spitsbergen  
649 (Worsley and Mørk, 2001; Luo, 2014; Luo et al., 2016). Middle Triassic *Rhizocorallium* from  
650 Luoping and other regions of the world (e.g. northwestern British Columbia) have comparable  
651 size ranges to their Spathian counterparts (e.g. Zonneveld et al., 2010; Fig. 9B). Burrow sizes  
652 of *Thalassinoides* also show obvious increases. Lower Triassic occurrences of *Thalassinoides*  
653 from Griesbachian strata of Northern Italy, Western Canada, Smithian strata at Susong in  
654 South China, and Spathian strata at Yashan (China) and the Western United States have  
655 burrow diameters less than 25 mm (e.g. Zonneveld et al., 2010; Hofmann et al., 2011; Pruss  
656 and Bottjer, 2004; Chen et al., 2011; Luo, 2014). The average values for these localities are  
657 less than 12 mm (Fig. 9C). At Luoping, the maximum burrow diameter of *Thalassinoides*  
658 reaches 30 mm, with the average diameter increasing to 17.9 mm. These values are similar to,  
659 or even greater than their Middle to Late Permian counterparts (Whidden, 1990; Zhao and  
660 Tong, 2010; Lima and Netto, 2012), and Middle Triassic *Thalassinoides* from north-eastern  
661 British Columbia (e.g. Zonneveld et al., 2010; Fig. 9C). In summary, the moderate to high  
662 ichnodiversity (nine ichnogenera) in the subtidal environments at Luoping, together with  
663 moderate to high bioturbation indices, the appearance of key ichnotaxa and increases in burrow  
664 sizes, represent a recovery stage four, which suggests a more or less fully recovered  
665 ichnossemblage in the early Middle Triassic, 7 Myr after the PTME.

666 It is worth noting that the bioturbation levels in the turbidite deposits in offshore settings  
667 are much higher than their surrounding non-turbiditic strata. In addition, various traces, such  
668 as *Diplocraterion*, *Planolites*, *Rhizocorallium*, *Sinusichnus*, *Taenidium*, and *Thalassinoides*  
669 were found in those beds. Certain traces, such as *Taenidium*, have penetrated sediments to a  
670 depth of 5 cm. Such moderate ichnoassemblages and moderate to high bioturbation levels in  
671 turbidite beds are interpreted to be the result of the short colonization of transported infaunal  
672 animals from proximal settings (*cf.* Grimm and Föllmi, 1994). The low ichnodiversity and low  
673 bioturbation level in non-turbiditic strata of offshore environments at Luoping are most likely

674 due to shallow marine anoxia, and this prevents further comparisons and discussion of their  
675 implications for recovery of trace makers in such distal shallow marine settings.

676 The offshore transition of Unit C in the Luoping sections is associated with low  
677 ichnodiversity and moderate bioturbation indices (BI), which is in contrast to the habitable  
678 zone model stating that the lower shoreface to offshore transition zone are ideal for  
679 colonization (*cf.* Beatty et al., 2008). The low ichnodiversity and moderate BI in the offshore  
680 transition at Luoping could partly relate to the topography of the basin and also its proximity  
681 to anoxic offshore settings. Several intraplatform basins were formed during the early Middle  
682 to Late Triassic at Luoping and its border areas, where well-preserved faunas were discovered  
683 (e.g. Hu et al, 2011; Benton et al., 2013). The restricted circulation and density stratification  
684 of the water column in these basins means they are not large in scale, and the shelf region in  
685 these basins could be narrow and steep. Such bathymetric topography prevented the  
686 development of a habitable zone and long-term colonization (*cf.* Zonneveld et al., 2010). In  
687 addition, the proximity of the offshore transition to the anoxic offshore setting at Luoping  
688 might also have hampered the bioturbating activities of trace makers in this environmental  
689 setting through possible upwelling of deeper anoxic waters.

690

### 691 *5.3. Implications for ichnofaunal recovery during the Early Triassic*

692

693 Investigations at Luoping support the utility of trace fossils to study the timing of biotic  
694 recovery and the processes of trace makers. The subtidal ichnoassemblage is characterized by  
695 medium to high ichnodiversity, medium to high bioturbation indices, and a marked increase in  
696 burrow size of many traces. These parameters, together with the common appearance of key  
697 ichnogenera (e.g. *Rhizocorallium* and *Thalassinoides*), suggests a recovery stage 4 (*sensu*  
698 Twitchett, 2006; Pietsch and Bottjer, 2014), thus indicating a full recovery of trace makers in  
699 subtidal environments. Ichnological records from adjacent regions also support an obvious  
700 recovery of trace makers (Feng et al., 2017c). In contrast, ichnological parameters from  
701 regional ichnoassemblages of Lower Triassic successions typically suggest a recovery stage  
702 of one and two, with a few data suggesting some recovery until the latest Smithian and  
703 Spathian (Twitchett, 1999; Chen et al., 2011; Zhao et al., 2015; Luo et al., 2016; Feng et al.,  
704 2017a). However, the ichnological parameters from offshore environments at Luoping show  
705 no signs of recovery. This is most likely due to the periodic anoxic bottom water conditions,  
706 which would have substantially inhibited the colonization of infaunal animals, but otherwise  
707 aided the fine preservation of the Luoping Biota.

708 After the PTME, marine ecosystems and ecological structures were re-shaped, with the  
709 Modern Evolutionary Fauna expanding to dominate in marine settings (Sepkoski et al., 1981;  
710 Erwin, 2006; Peters, 2008). The fossil composition of the Luoping Biota highlights this major  
711 change, with fishes, marine reptiles and decapod crustaceans comprising the majority of the  
712 fossil collections (e.g. Hu et al., 2011; Wen et al., 2012, 2013; Feldmann et al., 2012, 2015;  
713 Huang et al., 2013; Schweitzer et al., 2014). Luoping has revealed many new genera and  
714 species of arthropods, which suggest a radiation event during the early Middle Triassic (e.g.  
715 Feldmann et al., 2012, 2015, 2017; Huang et al., 2013; Schweitzer et al., 2014). Such a  
716 change in ecosystem structure was mirrored by the common occurrence of burrow systems  
717 (e.g. *Sinusichnus*, *Rhizocorallium*, *Spongeliomorpha*, and *Thalassinoides*) made by decapod  
718 crustaceans at Luoping. This highlights how the trace fossil assemblages of the early Middle  
719 Triassic document the major faunal changes occurring at this time in comparison with Lower  
720 Triassic ichnological records.

721

722

## 723 **6. Conclusions**

724

725

726 Well-preserved vertebrates and invertebrates from the Luoping Biota of Yunnan  
727 Province in South China suggest a stable, fully recovered shallow marine ecosystem in the  
728 early Middle Triassic (Anisian). Equally, well-preserved trace fossils found in association  
729 with the Luoping Biota provide a template to compare the behaviours and ecological  
730 strategies of trace-making organisms from such a recovered ecosystem with those in the  
731 delayed recovery interval of the Early Triassic. Trace fossil assemblages from the Luoping  
732 Biota have high ichnodiversity, with 14 ichnogenera discovered in the shallow marine  
733 environment of an intra-carbonate platform basin. Nine ichnogenera occurred in the subtidal  
734 environment. Such medium to high ichnodiversity, together with a marked increase in burrow  
735 size and the common occurrence of key ichnotaxa (e.g. *Rhizocorallium* and *Thalassinoides*)  
736 suggest a recovery stage of four. In contrast, non-turbiditic strata of the offshore setting record  
737 only three ichnogenera, with bioturbation indices never exceeding one. Periodic anoxic  
738 bottom water conditions are identified as the main control on such a protracted trace fossil  
739 record, which otherwise aided the fine preservation of body fossils of the Luoping Biota.  
740 Furthermore, event sedimentation (turbidites) in offshore settings host a medium  
741 ichnodiversity and medium bioturbation indices, both interpreted to result from short term

742 colonization by transported infaunal animals from proximal settings. The occurrence of  
743 variable crustacean-made traces (e.g. *Sinusichnus*, *Spongiomorpha*, and *Thalassinoides*) at  
744 Luoping, together with possible evidence of the decapod radiation from body fossils,  
745 highlights the value of using trace fossils to document ecosystem restructuring after the  
746 PTME.

747

## 748 **Acknowledgments**

749

750 This study was partly supported by the ACRDP discovery grant to G. R. Shi  
751 (DP150100690). This research is also supported by two NSFC grants (41572091 and  
752 41772007 to ZQC), two research grants (GBL21410, GPMR201601 to ML) from the State  
753 Key Laboratory of Biogeology and Environmental Geology, and State Key Laboratory of  
754 Geological Process and Mineral Resources, China University of Geosciences (Wuhan), and  
755 China Geological Survey project (DD20160020, 1212011140051, 12120114030601, and  
756 1212010610211). This paper is a contribution to the IGCP 630 “Permian-Triassic climatic and  
757 environmental extremes and biotic response”.

758

759

## 760 **References**

761

- 762 Abbassi, N., 2007. Shallow marine trace fossils from Upper Devonian sediments of the Kuh-E  
763 Zard, Zefreh area, central Iran. *Iranian Journal of Science & Technology, Transaction A*,  
764 31, 23–33.
- 765 Allison, P.A., Briggs, D.E.G., 1991. Taphonomy of non-mineralized tissues. In: Allison, P.A.,  
766 Briggs, D.E.G. (Eds.), *Taphonomy: Releasing the Data Locked in the Fossil Record*.  
767 Plenum Press, New York, 25–69.
- 768 Anderson, A., 1976. Fish trails from the Early Permian of South Africa. *Palaeontology* 19,  
769 397–409.
- 770 Bai, J.K., Yin, F.G., Zhang, Q.Y., 2011. Microfacies and enrichment pattern of fossils in the  
771 fossiliferous beds of Luoping Biota, Yunnan Province. *Geology in China*, 38, 393–402  
772 (in Chinese with English abstract).
- 773 Baucon, A., Carvalho, C.N.D., 2016. Stars of the aftermath: *Asteriacites* beds from the Lower  
774 Triassic of the Carnic Alps (Werfen Formation, Sauris Di Sopra), Italy. *Palaios* 31, 161–  
775 176.



- 776 Beatty, T.W., Zonneveld, J.P., Henderson, C.M., 2008. Anomalously diverse Early Triassic  
777 ichnofossil assemblages in northwest Pangea: a case for shallow-marine habitable zone.  
778 *Geology* 36, 771–774.
- 779 Belaústegui, Z., de Gibert, J.M., Lopez-Blanco, M., Bajo, I., 2014. Recurrent constructional  
780 pattern of the crustacean burrow *Sinusichnus sinuosus* from the Paleogene and Neogene  
781 of Spain. *Acta Palaenotol. Pol.* 59, 461–474.
- 782 Benner, J.S., Ridge, J.C., Knecht, R.J., 2009. Timing of post-glacial reinhabitation and  
783 ecological development of two New England, USA, drainages based on trace fossil  
784 evidence. *Palaeogeogr. Palaeoclimatol. Palaeoecol.* 272, 212–231.
- 785 Benton, M.J., Zhang, Q.Y., Hu, S.X., Chen, Z.Q., Wen, W., Liu, J., Huang, J.Y., Zhou, C.Y.,  
786 Xie, T., Tong, J.N., Choo, B., 2013. Exceptional vertebrate biotas from the Triassic of  
787 China, and the expansion of marine ecosystems after the Permo-Triassic mass extinction.  
788 *Earth-Sci. Rev.* 125, 199–243.
- 789 Bradshaw, M.A., 1981. Palaeoenvironmental interpretations and systematics of Devonian  
790 trace fossils from the Taylor Group (Lower Beacon Supergroup), Antarctica. *New  
791 Zealand J. Geol. Geophysics*, 24, 615–652.
- 792 Bradshaw, M.A., 2010. Devonian trace fossils of the Horlick Formation, Ohio Range,  
793 Antarctica: systematic description and palaeoenvironmental interpretation. *Ichnos* 17, 58–  
794 114.
- 795 Bromley, R.G., 1996. *Trace Fossils. Biology, Taphonomy and Applications*. London:  
796 Chapman & Hall. 361 pp.
- 797 Bromley, R.G., Asgaard, U., 1979. Triassic freshwater ichnocoenoses from Carlsberg Fjord,  
798 East Greenland. *Palaeogeogr. Palaeoclimatol. Palaeoecol.* 28, 39–80.
- 799 Bromley, R.G., Frey, R.W., 1974. Redescription of the trace fossil *Gyrolithes* and taxonomic  
800 evaluation of *Thalassinoides*, *Ophiomorpha* and *Spongeliomorpha*. *Bull. Geol. Soc.  
801 Denmark* 23, 311–335.
- 802 Buatois, L.A., Mángano, M.G., 2002. Trace fossils from Carboniferous floodplain deposits in  
803 western Argentina: implications for ichnofacies models of continental environments.  
804 *Palaeogeogr. Palaeoclimatol. Palaeoecol.* 183, 71–86.
- 805 Buatois, L.A., Mángano, M.G., 2011a. *Ichnology: Organism-Substrate Interaction in Space  
806 and Time*. Cambridge University Press, New York, 358 pp.
- 807 Buatois, L.A., Mángano, M.G., 2011b. The déjà vu effect: recurrent patterns in exploitation of  
808 ecospace, establishment of the mixed layer, and distribution of matgrounds. *Geology* 39,  
809 1163–1166.

- 810 Buatois, L.A., Mángano, M.G., 2013. Ichnodiversity and ichnodisparity: significance and  
811 caveats. *Lethaia* 46, 281–292.
- 812 Buatois, L.A., Macsotay, O., Quiroz, L.I., 2009. *Sinusichnus*, a trace fossil from Antarctica and  
813 Venezuela: expanding the datasets of crustacean burrows. *Lethaia* 42, 511–518.
- 814 Buckman, J.O., 1994. *Archaeonassa* Fenton and Fenton 1937 reviewed. *Ichnos* 3, 185–192.
- 815 Bustillo, M.A., Ruiz-Ortiz, P.A., 1987. Chert occurrence in carbonate turbidites: example  
816 from the Upper Jurassic of the Betic Mountains (southern Spain). *Sedimentology* 34,  
817 611–621.
- 818 Carmona, N.B., Buatois, L.A., Mángano, M.G., 2004. The trace fossil record of burrowing  
819 decapod crustaceans: evaluating evolutionary radiations and behavioural convergence.  
820 *Fossil and Strata* 51, 141–153.
- 821 Carvalho, C.N.D., Viegas, P.A., Cachão, M., 2007. *Thalassinoides* and its producer:  
822 populations of *Mecochirus* buried within their burrow system, Boca Do Chapim  
823 Formation (Lower Cretaceous), Portugal. *Palaios* 22, 104–109.
- 824 Chen, Z.Q., Benton, M.J., 2012. The timing and pattern of biotic recovery following the end-  
825 Permian mass extinction. *Nat. Geosci.* 5, 375–383.
- 826 Chen, Z.Q., Fraiser, M.L., Bolton, C., 2012. Early Triassic trace fossils from Gondwana  
827 Interior Sea: Implication for ecosystem recovery following the end-Permian mass  
828 extinction in south high-latitude region. *Gondwana Res.* 22, 238–255.
- 829 Chen, Z.Q., Tong, J.N., Fraiser, M.L., 2011. Trace fossil evidence for restoration of marine  
830 ecosystems following the end-Permian mass extinction in the Lower Yangtze region,  
831 South China. *Palaeogeogr. Palaeoclimatol. Palaeoecol.* 299, 449–474.
- 832 Chen, Z.Q., Yang, H., Luo, M., Benton, M.J., Kaiho, K., Zhao, L.S., Huang, Y.G., Zhang,  
833 K.X., Fang, Y.H., Jiang, H.S., Qiu, H., Li, Y., Tu, C.Y., Shi, L., Zhang, L., Feng, X.Q.,  
834 Chen, L., 2015. Complete biotic and sedimentary records of the Permian-Triassic  
835 transition from Meishan section, South China: ecologically assessing mass extinction and  
836 its aftermath. *Earth Sci. Rev.* 149, 67–107.
- 837 D’Alessandro, A., Bromley, R.G., 1987. Meniscate trace fossils and the *Muensteria*-  
838 *Taenidium* problem. *Palaeontology* 30, 743–763.
- 839 Ding, Y., Cao, C.Q., Zheng, Q.F., 2016. Lopingian (Upper Permian) trace fossils from the  
840 northern Penglaitan Section, Laibin, Guangxi, South China and their environmental  
841 implications. *Palaeoworld* 25, 377–387.
- 842 Dott, R.H., Bourgeois, J., 1982. Hummocky stratification: significance of its variable bedding  
843 sequences. *Geol. Soc. Am. Bull.* 93, 663–680.

844 Dumas, S., Arnott, R.W.C. 2006. Origin of hummocky and swaley cross-stratification—the  
845 control influence of unidirectional current strength and aggradation rate. *Geology* 34,  
846 1073–1075.

847 Enos, P., Lehrmann, D.J., Wei, J.Y., Yu, Y.Y., Xiao, J.F., Chaikin, D.H., Minzoni, M., Berry,  
848 A.K., Montgomery, P., 2006. Triassic Evolution of the Yangtze Platform in Guizhou  
849 Province, People’s Republic of China. *Geol. Soc. Am. Special Papers* 417, 1–105.

850 Erwin, D.H., Bowring, S.A., Jin, Y.G., 2002. End-Permian mass extinction: a review. In:  
851 Koeberl, C., MacLeod, K.G. (Eds.), *Catastrophic events and Mass Extinctions: Impacts*  
852 *and Beyond*. *Geol. Soc. Am. Special Paper* 256, pp. 353–383.

853 Erwin, D.H., 2006. *Extinction: How Life on Earth Nearly Ended 250 Million Years Ago*.  
854 Princeton University Press, Princeton, 296 pp.

855 Ezaki, Y., Liu, J.B., Nagano, T., Adachi, N., 2008. Geobiological aspects of the earliest  
856 Triassic microbialites along the southern periphery of the tropical Yangtze Platform:  
857 initiation and cessation of a microbial regime. *Palaios* 23, 356–369.

858 Ezaki, Y., Liu, J.B., Adachi, N., 2012. Lower Triassic stromatolites in Luodian County,  
859 Guizhou Province, South China: evidence for the protracted devastation of the marine  
860 environments. *Geobiology* 10, 48–59.

861 Feldmann, R.M., Schweitzer, C.E., Hu, S.X., Zhang, Q.Y., Zhou, C.Y., Xie, T., Huang, J.Y.,  
862 Wen, W., 2012. Macrurous Decapoda from the Luoping biota (Middle Triassic) of China.  
863 *J. Paleontol.* 86, 425–441.

864 Feldmann, R.M., Schweitzer, C.E., Hu, S.X., Huang, J.Y., Zhou, C.Y., Zhang, Q.Y., Wen,  
865 W., Xie, T., Maguire, E., 2015. Spatial distribution of Crustacea and associated organisms  
866 in the Luoping biota (Anisian, Middle Triassic), Yunnan Province, China: evidence of  
867 periodic mass kills. *J. Paleontol.* 89, 1022–1037.

868 Feng, X.Q., Chen, Z.Q., Woods, A., Fang, Y.H., 2017a. A Smithian (Early Triassic)  
869 ichnoassemblage from Lichuan, Hubei Province, South China: implications for biotic  
870 recovery after the latest Permian mass extinction. *Palaeogeogr. Palaeoclimatol.*  
871 *Palaeoecol.* 486, 123–141.

872 Feng, X.Q., Chen, Z.Q., Bottjer, D.J., Fraiser, M.L., Xu, Y.L., Luo, M., 2017b. Additional  
873 records of ichnogenus *Rhizocorallium* from the Lower and Middle Triassic, south China:  
874 implications for biotic recovery after the end-Permian mass extinction. *GSA Bull.* (in  
875 press).

876 Feng, X.Q., Chen, Z.Q., Woods, A., Wu, S.Q., Fang, Y.H., Luo, M., Xu, Y.L., 2017c. Anisian  
877 (Middle Triassic) marine ichnocoenoses from the eastern and western margins of the

878 Kamdian Continent, Yunnan Province, SW China: implications for the Triassic biotic  
879 recovery. *Glob. Planet. Chang.* 157, 194–213.

880 Feng, Z.Z., Bao, Z.D., Li, S.W., 1997. Lithofacies paleogeography of Middle and Lower  
881 Triassic of South China. Petroleum Industry Press, Beijing, pp. 1–222 (in Chinese with  
882 English abstract).

883 Fenton, C.L., Fenton, M.A., 1937. *Archaeonassa*, Cambrian snail trails and burrows.  
884 *American Midland Naturalist* 18, 454–456.

885 Fillmore, D.L., Lucas, S.G., Simpson, E.L., 2011. The fish swimming trace *Undichna* from  
886 the Mississippian Mauch Chunk Formation, Eastern Pennsylvania. *Ichnos* 18, 27–34.

887 Flügel, E., 2004. Microfacies of carbonate rocks: analysis, interpretation and application.  
888 Springer, New York, pp. 1–976.

889 Foster, W.J., Twitchett, R.J., 2014. Functional diversity of marine ecosystems after the Late  
890 Permian mass extinction event. *Nat. Geosci.* 7, 233–238

891 Fraiser, M.L., Bottjer, D.J., 2009. Opportunistic behavior of invertebrate marine tracemakers  
892 during the Early Triassic aftermath of the end-Permian mass extinction. *Aust. J. Earth  
893 Sci.* 56, 841–857.

894 Gibert, J.M.de., 2001. *Undichna gosiutensis*, isp. nov.: a new fish trace fossil from the  
895 Jurassic of Utah. *Ichnos* 8, 15–22.

896 Gibert, J.M.de., Martinell, J., 1996. Trace fossil assemblages and their palaeoenvironmental  
897 significance in the Pliocene marginal marine deposits of the Baix Ebre (Catalonia, NE  
898 Spain). *Géologie Méditerranéenne* 23, 211–225.

899 Gibert, J.M.de., 1996. A new decapod burrow system from the NW Mediterranean Pliocene.  
900 *Revista Española de Paleontología* 11, 251–254.

901 Gibert, J.M.de., Jeong, K., Martinell, J. 1999a. Ethologic and ontogenic significance of the  
902 Pliocene trace fossil *Sinusichnus sinuosus* from the northwestern Mediterranean. *Lethaia*  
903 32, 31–40.

904 Gibert, J.M.de., Buatois, L.A., Fregenal-Martinez, M.A., Mangano, M.G., Ortega, F., Poyato-  
905 Ariza, F.J., Wenz, S., 1999b. The fish trace fossil *Undichna* from the Cretaceous of  
906 Spain. *Palaeontology* 42, 409–427.

907 Godbold, A., Schoepfer, S., Shen, S.Z., Henderson, C.M., 2017. Precarious ephemeral  
908 refugia during the earliest Triassic. *Geology* 45, 607–610.

909 Graham, J.R., Pollard, J.E., 1982. Occurrence of the trace fossil *Beaconites antarcticus* in the  
910 lower Carboniferous fluviatile rocks of county Mayo, Ireland. *Palaeogeogr.  
911 Palaeoclimatol. Palaeoecol.* 38, 257–268.

- 912 Grimm, K.A., Follmi, K.B., 1994. Doomed pioneers: allochthonous crustacean tracemakers in  
913 anaerobic basinal strata, Oligo-Miocene San Gregorio Formation, Baja California Sur,  
914 Mexico. *Palaios* 9, 313–334.
- 915 Hall, J., 1847. Paleontology of New York. Volumn 1, C. Van Benthuyzen, Albany, 362 pp.
- 916 Häntzschel, W., 1975. Trace fossil and Problematica. In: Teichert, C. (ed.), *Treatise on*  
917 *Invertebrate Paleontology, Part W, Miscellanea, Supplement I*, Geological Society of  
918 America and University of Kansas Press, pp. 1–269.
- 919 Heer, O., 1877. *Flora Fossilis Helvetiae. Vorweltliche Flora der Schweiz*. J. Wurster &  
920 Comp., Zurich, 182 pp.
- 921 Hofmann, R., Goudemand, N., Wasmer, M., Bucher, H., Hautmann, M., 2011. New trace  
922 fossil evidence for an early recovery signal in the aftermath of the end-Permian mass  
923 extinction. *Palaeogeogr. Palaeoclimatol. Palaeoecol.* 310, 216–226.
- 924 Hofmann, R., Buatois, L.A., MacNaughton, R.B., Mangano, M.G., 2015. Loss of sedimentary  
925 mixed layer as a result of the end-Permian extinction. *Palaeogeogr. Palaeoclimatol.*  
926 *Palaeoecol.* 428, 1–11.
- 927 Hu, S.L., Li, Y.J., Dai, M., Pu, Z.P., 1996. The laser mass-spectrometer  $^{40}\text{Ar}$ – $^{49}\text{Ar}$  age of  
928 green pisolites of Guizhou Province. *Acta Petrol. Sin.* 12, 409–415 (in Chinese).
- 929 Hu, S.X., Zhang, Q.Y., Chen, Z.Q., Zhou, C.Y., Lv, T., Xie, T., Wen, W., Huang, J.Y.,  
930 Benton, M.J., 2011. The Luoping biota: exceptional preservation, and new evidence on  
931 the Triassic recovery from end-Permian mass extinction. *Proc. R. Soc. B* 278, 2274–  
932 2283.
- 933 Huang, J.Y., Feldmann, R.M., Schweitzer, C.E., Hu, S.X., Zhou, C.Y., Benton, M.J., Zhang,  
934 Q.Y., Wen, W., Xie, T., 2013. A new shrimp (Decapoda, Dendrobranchiata, Penaeoidea)  
935 from the Middle Triassic of Yunnan, Southwest China. *J. Paleont.* 87, 603–611.
- 936 Huang, J.Y., Zhang, K.X., Zhang, Q.Y., Lv, T., Zhou, C.Y., Bai, J.K., 2009. Conodonts  
937 stratigraphy and sedimentary environment of the Middle Triassic at Daozi Section of  
938 Luoping county, Yunnan province, South China. *Acta Micropalaeontologica Sinica* 26,  
939 211–224 (In Chinese with English abstract).
- 940 Hull, P., Darroch, S.A.F., 2013. Mass extinction and the structure and function of ecosystem.  
941 In: Bush, A., Pruss, S.B., Payne, J.L. (Eds.), *Ecosystem Paleobiology and Geobiology*,  
942 The Paleontological Society Papers 19, 1–42.
- 943 Jame, N.P., Bourque, P.A., 1992. Reefs and Mounds. In: Walker, R.G., James, N.P (Eds.),  
944 *Facies Models: response to sea level change*. Geological Association of Canada, St.  
945 John's, pp. 323–348.

946 Keighley, D.G., Pickerill, R.K., 1994. The ichnogenus *Beaconites* and its distinction from  
947 *Ancorichnus* and *Taenidium*. *Palaeontology* 37, 305–337.

948 Knaust, D., 2007. Invertebrate trace fossils and ichnodiversity in shallow-marine carbonates  
949 of the German Middle Triassic (Muschelkalk). In: Bromley, R.G., Buatois, L.A.,  
950 Mangano, G., Genise, J.F., Melchor, R.N., (Eds.), *Sediment-Organism Interactions: a*  
951 *multifaceted ichnology*. SEPM Special Publication 88, pp. 223–240.

952 Knaust, D., 2010. The end-Permian mass extinction and its aftermath on an equatorial  
953 carbonate platform: insights from ichnology. *Terra Nova* 22, 195–202.

954 Knaust, D., 2013. The ichnogenus *Rhizocorallium*: classification, trace makers,  
955 palaeoenvironments and evolution. *Earth Sci. Rev.* 126, 1–47.

956 Knaust, D., Uchman, A., Hagdorn, H., 2016. The probable isopod burrow *Sinusichnus*  
957 *seilacheri* isp. n. from the Middle Triassic of Germany: an example of behavioural  
958 convergence. *Ichnos* 24, 138–146.

959 Kotake, N., 1992. Deep-sea echiurans: possible producers of *Zoophycos*. *Lethaia* 25, 311–316.

960 Książkiewicz, M., 1968. O niektórych problematykach z fliszKarpát polskich, Część III.  
961 *Rocznik Polskiego Towarzystwa Geologicznego* 38, 3–17.

962 Książkiewicz, M., 1977. Trace fossils in the flysch of the Polish Carpathians. *Palaeontol. Pol.*  
963 36, 1–208.

964 Lehrmann, D.J., Enos, P., Payne, J.L., Montgomery, P., Wei, J.Y., Yu, Y.Y., Xiao, J.F.,  
965 Orchard, M.J., 2005. Permian and Triassic depositional history of the Yangtze platform  
966 and Great Bank of Guizhou in the Nanpanjiang Basin of Guizhou and Guangxi, South  
967 China. *Albertiana* 33, 149–168.

968 Lima, J.H., Netto, R.G., 2012. Trace fossils from the Permian Teresina Formation at Cerro  
969 Caveiras (S Brazil). *Revista Brasileira de Paleontology* 15, 5–22.

970 Liu, J., Hu, S.X., Rieppel, O., Jiang, D.Y., Benton, M.J., Kelley, N.P., Aitchison, J.C., Zhou,  
971 C.Y., Wen, W., Huang, J.Y., Xie, T., Lv, T., 2014. A gigantic nothosaur (Reptilia:  
972 Sauropterygia) from the Middle Triassic of SW China and its implication for the Triassic  
973 biotic recovery. *Sci. Rep.* 4, e7142.

974 Luo, M., 2014. Early Triassic trace fossils from South China: implications for biotic recovery  
975 from the end-Permian Mass Extinction. The University of Western Australia.  
976 Unpublished PhD thesis. 1–222.

977 Luo, M., Chen, Z.Q., 2014. New arthropod traces from the Lower Triassic Kockatea Shale  
978 Formation, northern Perth Basin, Western Australia: ichnology, taphonomy and  
979 palaeoecology. *Geological J.* 49, 163–176.

- 980 Luo, M., Chen, Z.Q., Hu, S.X., Zhang, Q.Y., Benton, M.J., Zhou, C.Y., Wen, W., Huang,  
981 J.Y., 2013. Carbonate reticulated ridge structures from the lower Middle Triassic of the  
982 Luoping area, Yunnan, southwestern China: Geobiologic features and implications for  
983 exceptional preservation of the Luoping Biota. *Palaios* 28, 541–551.
- 984 Luo, M., George, A.D., Chen, Z.Q., 2016. Sedimentology and ichnology of two Lower  
985 Triassic sections in South China: implications for the biotic recovery from the end-  
986 Permian Mass extinction. *Glob. Planet. Chang.* 144, 198–212.
- 987 Luo, M., Hu, S.X., Benton, M.J., Zhao, L.S., Huang, J.Y., Song, H.J., Wen, W., Zhang, Q.Y.,  
988 Fang, Y.H., Huang, Y.G., Chen, Z.Q., 2017. Taphonomy and palaeobiology of early  
989 Middle Triassic coprolites from the Luoping biota, southwest China: implications for  
990 reconstruction of fossil food webs. *Palaeogeogr. Palaeoclimatol. Palaeoecol.* 474, 223–  
991 246.
- 992 MacEachern, J.A., Bann, K.L., Gingras, M.K., Zonneveld, J.P., Dashtgard, S.E., Pemberton,  
993 S.G., 2012. The ichnofacies paradigm. In: Knaust, D., Bromley, R.G., (Eds.), *Trace*  
994 *Fossils as Indicators of Sedimentary Environments. Developments in Sedimentology* 64,  
995 103–138.
- 996 MacEachern, J.A., Bann, K.L., Pemberton, S.G., Gingras, M.K., 2007. The ichnofacies  
997 paradigm: high resolution paleoenvironmental interpretation of the rock record. In:  
998 MacEachern, J.A., Gingras, M.K., Pemberton, S.G. (Eds.), *Applied Ichnology. SEPM*  
999 *Short Course Notes* 52, 27–46.
- 1000 Massalongo, A., 1855. *Zoophycos*, novum genus plantorum fossilium. Antonelli, Verona, 52  
1001 pp.
- 1002 Mata, S.C., Bottjer, D.J., 2011. Origin of Lower Triassic microbialites in mixed carbonate–  
1003 siliciclastic successions: ichnology, applied stratigraphy, and the end-Permian mass  
1004 extinction. *Palaeogeogr. Palaeoclimatol. Palaeoecol.* 300, 158–178.
- 1005 McBride, E.F., Folk, R.L., 1979. Features and origin of Italian Jurassic radiolarites deposited  
1006 on continental crust. *J. Sediment. Petrol.* 49, 838–868.
- 1007 McGhee, G.R., Sheehan, P.M., Bottjer, D.J., Droser, M.L., 2004. Ecological ranking of  
1008 Phanerozoic biodiversity crises: ecological and taxonomic severities are decoupled.  
1009 *Palaeogeogr. Palaeoclimatol. Palaeoecol.* 211, 289–297.
- 1010 Melchor, R.N., Bromley, R.G., Bedatou, E., 2009. *Spongeliomorpha* in nonmarine settings: an  
1011 ichnotaxonomic approach. *Earth Environment. Sci. Trans. R. Soc. Edinburgh* 100, 429–  
1012 436.

- 1013 Morrissley, L.B., Braddy, S.J., S.J., Bennett, J.P., Marriott, S.B., Tarrant, P.R., 2004. First  
1014 trails from the Lower Old Red Sandstone of Tredomen Quarry, Powys, southeast Wales.  
1015 Geological J. 38, 337–358.
- 1016 Morrow, J.R., Hasiotis, S.T., 2007. Endobenthic response through mass extinction episodes:  
1017 predictive models and observed patterns. In: Miller III, W. (Ed.), Trace Fossils: Concepts,  
1018 Problems, Prospects. Elsevier, Amsterdam, pp. 575–598.
- 1019 Myrow, P.M., 1995. *Thalassinoides* and the enigma of early Paleozoic open-framework  
1020 burrow systems. *Palaios* 10, 58–74.
- 1021 Nicholson, H.A., 1873. Contributions to the study of the errant annelids of the older  
1022 Palaeozoic rock. *Proc. R. Soc. London*. 21, 288–290.
- 1023 Olóriz, F., Rodríguez-Tovar, F.J., 2000. *Diplocraterion*: A useful marker for sequence  
1024 stratigraphy and correlation in the Kimmeridgian, Jurassic (Prebetic Zone, Betic  
1025 Cordillera, southern Spain). *Palaios* 15, 546–552.
- 1026 Osgood, R.G., 1970. Trace fossils of the Cincinnati area. *Palaeontographica Americana*, 6,  
1027 277–444.
- 1028 Pemberton, S.G., Frey, R.W., 1982. Trace fossil nomenclature and the  
1029 *Planolites–Palaeophycus* dilemma. *J. Paleontol.* 56, 843–881.
- 1030 Peters, S.E., 2008. Environmental determinants of extinction selectivity in the fossil record.  
1031 *Nature* 454, 626–629.
- 1032 Pietsch, C., Bottjer, D.J., 2014. The importance of oxygen for the disparate recovery patterns  
1033 of the benthic macrofauna in the Early Triassic. *Earth Sci. Rev.* 137, 65–84.
- 1034 Pruss, S.B., Bottjer, D.J., 2004. Early Triassic trace fossils of the Western United States and  
1035 their implications for prolonged environmental stress from the end-Permian Mass  
1036 Extinction. *Palaios* 19, 551–564.
- 1037 Reineck, H.E., 1963. Sedimentgefüge im Bereich der südliche Nordsee. *Abhandlungen*  
1038 *Senckenbergischen Naturforschende Gesellschaft*, 505, 1–138.
- 1039 Schweitzer, C.E., Feldmann, R.M., Hu, S.X., Huang, J.Y., Zhou, C.Y., Zhang, Q.Y., Wen,  
1040 W., Xie, T., 2014. Penaeoid Decapoda (Dendrobranchiata) from the Luoping biota  
1041 (Middle Triassic) of China: systematics and taphonomic framework. *J. Paleontol.* 88,  
1042 457–474.
- 1043 Seilacher, A., 1974. Flysch trace fossils: evolution of behavioural diversity in the deep-sea.  
1044 *Neues Jahrbuch für Geologie und Paläontologie, Monatshefte* 4, 233–245.
- 1045 Sepkoski, J.J., Bambach, R.K., Raup, D.M., Valentine, J.W., 1981. Phanerozoic marine  
1046 diversity and the fossil record. *Nature*, 293, 435–437.



- 1047 Shi, G., Woods, A., Yu, M.Y., Wei, H.Y., 2015. Two episodes of evolution of trace fossils  
1048 during the Early Triassic in the Guiyang area, Guizhou Province, South China.  
1049 *Palaeogeogr. Palaeoclimatol. Palaeoecol.* 426, 275–284.
- 1050 Sperling, E.A., 2013. Tackling the 99%: can we begin to understand the paleoecology of the  
1051 small and soft-bodied animal majority? In: Bush, A., Pruss, S.B., Payne, J. (Eds.),  
1052 *Ecosystem Paleobiology and Geobiology. The Paleontological Society Papers* 19, 77–86.
- 1053 Stockar, R., 2010. Facies, depositional environment, and palaeoecology of the Middle Triassic  
1054 Cassina beds (Meride Limestone, Monte San Giorgio, Switzerland). *Swiss J. Geosci.* 103,  
1055 101–119.
- 1056 Taylor, A.M., Gawthorpe, R.L., 1993. Application of sequence stratigraphy and trace fossil  
1057 analysis to reservoir description: Examples from the Jurassic of the North Sea. In Parker,  
1058 J.R., ed., *Petroleum Geology of Northwest Europe: Proceedings of the 4th Conference:*  
1059 *Geological Society, London*, 317–335.
- 1060 Taylor, A.M., Goldring, R., 1993. Description and analysis of bioturbation and ichnofabric. *J.*  
1061 *Geol. Soc.* 150, 141–148.
- 1062 Torell, O.M., 1870. *Petrificata Suecana Formationis Cambricae. Lunds Universitets Årsskrift,*  
1063 6, 1–14.
- 1064 Twitchett, R.J., 1999. Palaeoenvironments and faunal recovery after the end-Permian Mass  
1065 Extinction. *Palaeogeogr. Palaeoclimatol. Palaeoecol.* 154, 27–37.
- 1066 Twitchett, R.J., 2006. The palaeoclimatology, palaeoecology and palaeoenvironmental  
1067 analysis of mass extinction events. *Palaeogeogr. Palaeoclimatol. Palaeoecol.* 232, 190–  
1068 213.
- 1069 Twitchett, R.J., Barras, C.G., 2004. Trace fossils in the aftermath of mass extinction events.  
1070 In: McIlroy, D. (Ed.), *Application of Ichnology to Palaeoenvironmental and Stratigraphic*  
1071 *Analysis: Geological Society of London, Special Publication*, 228, pp. 395–415.
- 1072 Twitchett, R.J., Wignall, P.B., 1996. Trace fossils and the aftermath of the Permo–Triassic  
1073 mass extinction: evidence from northern Italy. *Palaeogeogr. Palaeoclimatol. Palaeoecol.*  
1074 124, 137–151.
- 1075 Uchman, A., 1995. Taxonomy and palaeoecology of flysch trace fossils: The Marnoso-  
1076 arenacea Formation and associated facies (Miocene, Northern Apennines, Italy).  
1077 *Beringeria* 15, 1–115.
- 1078 Uchman, A., 1998. Taxonomy and ethology of flysch trace fossils: revision of the marian  
1079 Książkiewicz collection and studies of complementary materials. *Annales Societatis*  
1080 *Geologorum Poloniae* 68, 105–218.

- 1081 Uchman, A., Hanken, N. M., Nielsen, J. K., Grundvåg, S.A., Piasecki, S., 2016. Depositional  
1082 environment, ichnological features and oxygenation of Permian to earliest Triassic marine  
1083 sediments in central Spitsbergen, Svalbard. *Polar Res.* 35, e24782.
- 1084 Vossler, S.M., Pemberton, S.G., 1988. *Skolithos* in the Upper Cretaceous Cardium Formation:  
1085 an ichnofossil example of opportunistic ecology. *Lethaia* 21, 351–362.
- 1086 Walker, R.G., 1992. Turbidites and submarine fans. In: Walker, R.G., James, N.P (Eds.),  
1087 Facies Models: response to sea level change. Geological Association of Canada, St.  
1088 John's, pp. 239–264.
- 1089 Wen, W., Zhang, Q.Y., Hu, S.X., Zhou, C.Y., Xie, T., Huang, J.Y., Chen, Z.Q., Benton, M.J.,  
1090 2012. A new basal actinopterygian fish from the Anisian (Middle Triassic) of Luoping,  
1091 Yunnan Province, Southwest China. *Acta Palaeontol. Pol.* 57, 149–160.
- 1092 Wen, W., Zhang, Q.Y., Hu, S.X., Benton, M.J., Zhou, C.Y., Xie, T., Huang, J.Y., Chen, Z.Q.,  
1093 2013. Coelacanths from the Middle Triassic Luoping biota, Yunnan, South China, with  
1094 the earliest evidence of ovoviviparity. *Acta Palaeontol. Pol.* 58, 175–193.
- 1095 Whidden, K.J., 1990. Preferential silicification of trace and body fossils in the Fossil  
1096 Mountain Member of the Permian Kaibab Formation (southwestern Utah): Unpublished  
1097 M.S Thesis, University of Southern California, Los Angeles, 158 pp.
- 1098 Wignall, P.B., Hallam, A., Lai, X.L., Yang, F.Q., 1995. Palaeoenvironmental changes across  
1099 the Permian/Triassic boundary at Shangshi (N. Sichuan, China). *Historical Biol.* 10, 175–  
1100 189.
- 1101 Wignall, P.B., Morante, R., Newton, R., 1998. The Permo–Triassic transition in Spitsbergen:  
1102  $\delta^{13}\text{C}_{\text{org}}$  chemostratigraphy, Fe and S geochemistry, facies, fauna and trace fossils. *Geol.*  
1103 *Mag.* 135, 47–62.
- 1104 Wignall, P.B., Newton, R., 1998. Pyrite framboid diameter as a measure of oxygen deficiency  
1105 in ancient mudrocks. *Am. J. Sci.* 298, 537–552.
- 1106 Wilkin, R.T., Barnes, H.L., Brantley, S.L., 1996. The size distribution of framboidal pyrite in  
1107 modern sediments: an indicator of redox conditions. *Geochim. Cosmochim. Acta* 60,  
1108 3897–3912.
- 1109 Worsley, D., Mørk, A., 2001. The environmental significance of the trace fossil  
1110 *Rhizocorallium jenense* in the Lower Triassic western Spitsbergen. *Polar Res.* 20, 37–48.
- 1111 Yochelson, E.L., Fedonkin, M.A., 1997. The type specimens (Middle Cambrian) of the trace  
1112 fossil *Archaeonassa* Fenton and Fenton. *Can. J. Earth. Sci.* 34, 1210–1219.
- 1113 Zhang, Q.Y., Wen, W., Hu, S.X., Benton, M.J., Zhou, C.Y., Xie, T., Lu, T., Huang, J.Y.,  
1114 Choo, B., Chen, Z.Q., Liu, J., Zhang, Q.C., 2014. Nothosaur foraging tracks from the

1115 Middle Triassic of Southwestern China. *Nat. Commun.* 5, 3973e, DOI:  
1116 10.1038/ncomms4973.

1117 Zhang, Q.Y., Zhou, C.Y., Lu, T., Xie, T., Lou, X.Y., Liu, W., Sun, Y.Y., Wang, X.S., 2008a.  
1118 Discovery and significance of the Middle Triassic Anisian Biota. *Geol. Rev.* 54, 523–527  
1119 (in Chinese with English abstract).

1120 Zhang, Q.Y., Zhou, C.Y., Lu, T., Xie, T., Lou, X.Y., Liu, W., Sun, Y.Y., Huang, J.Y., Zhao,  
1121 L.S., 2009. A conodont-based Middle Triassic age assignment for the Luoping Biota of  
1122 Yunnan, China. *Science in China Series D: Earth Sciences* 52, 1673–1678.

1123 Zhang, L.J., Fan, R.Y., Gong, Y.M., 2015. *Zoophycos* macroevolution since 541 Ma. *Sci.*  
1124 *Rep.* 4, e14954.

1125 Zhang, X.H., Shi, G.R., Gong, Y.M., 2008b. Middle Jurassic trace fossils from the Ridang  
1126 Formation in Sajia County, South Tibet, and their palaeoenvironmental significance.  
1127 *Facies* 54, 45–60.

1128 Zhao, X.M., Tong, J.N., 2010. Two episodic changes of trace fossils through the Permian-  
1129 Triassic transition in the Meishan cores, Zhejiang Province. *Sci. China Ser. D Earth Sci.*  
1130 53, 1885–1893.

1131 Zhao, X.M., Tong, J.N., Yao, H.Z., Niu, Z.J., Luo, M., Huang, Y.F., Song, H.J., 2015. Early  
1132 Triassic trace fossils from the Three Gorges area of South China: implications for the  
1133 recovery of benthic ecosystems following the Permian-Triassic extinction. *Palaeogeogr.*  
1134 *Palaeoclimatol. Palaeoecol.* 429, 100–116.

1135 Zenker, J.C., 1836. *Historisch-topographisches Taschenbuch von Jena und seiner Umgebung.*  
1136 Friedrich Frommann, Jena. 1–338.

1137 Zonneveld, J.P., 2011. Suspending the rules: unravelling the ichnological significance of the  
1138 Lower Triassic post-extinction recovery interval. *Palaios* 26, 677–681.

1139 Zonneveld, J.P., Gingras, M.K., Pemberton, S.G., 2001. Trace fossil assemblages in a Middle  
1140 Triassic mixed siliciclastic–carbonate marginal marine coastal depositional system,  
1141 British Columbia. *Palaeogeogr. Palaeoclimatol. Palaeoecol.* 166, 249–276.

1142 Zonneveld, J.P., Gingras, M.K., Beatty, T.W., 2010. Diverse ichnofossil assemblage  
1143 following the P-T mass extinction, Lower Triassic, Alberta and British Columbia,  
1144 Canada: evidence for shallow marine refugia on the northwestern coast of Pangaea.  
1145 *Palaios* 25, 368–392.

1146

1147 **Figure and Figure captions**

1148

1149 Fig. 1.A, Location of the three studied sections (stars) at Luoping, Yunnan Province of South  
1150 China. Note the insert map (B) only shows mainland China. B, Middle Triassic  
1151 palaeogeographic map of South China showing the palaeogeographic setting of Luoping and  
1152 adjacent areas [base map modified from Feng et al., (1997)].

1153

1154 Fig. 2. Stratigraphic columns showing the distribution of trace fossils and bioturbation levels  
1155 of the three studied representative sections at Luoping, Yunnan Province. The bioturbation  
1156 scheme follows Reineck (1963) and Taylor and Goldring (1993). Abundant invertebrate and  
1157 vertebrate fossils occur in the Dawazi, Xiangdongpo, and Shangshikan sections, which are  
1158 abbreviated as DWZ, XDP, and SSK, respectively. Note, the nodular, bioturbated carbonate  
1159 wackestone is here applied as a marker bed to correlate the trace fossil records of the three  
1160 sections.

1161

1162 Fig. 3. Field photos showing the typical rock types and sedimentary structures within each  
1163 unit of the three sections. A, oncoidal packstone-wackestone, bed 2, XDP. Note the individual  
1164 oval to irregular shaped oncoids (arrowed); B, laminated marly carbonate mudstone, bed  
1165 26–27, SSK. Note the very thin-bedded chert layers (arrowed) intercalated in marly carbonate  
1166 mudstone. Hammer is 39 cm long; C, plan view of carbonate reticulated ridge structures. Bed  
1167 88, XDP; D, Turbidite deposits from the XDP section, bed 55. The sharp-based, normally  
1168 graded wacke-packstone layer is overlain by very thin layers of planar- to convolute-  
1169 laminated carbonate mudstone and structureless carbonate mudstone. They are here  
1170 interpreted to represent Ta, Tb+Tc and Te of the Bouma turbiditic sequence. E, nodular  
1171 carbonate wackestone and overlying marly carbonate mudstone. XDP, bed 73 and 74. F,  
1172 Hummocky cross-stratified carbonate wackestone; XDP, bed 136. G, thick-bedded carbonate  
1173 mudstone, with planar lamination. XDP, bed 167 and 168. H, laminated stromatolitic  
1174 dolomite, bed 187, DWZ.

1175

1176 Fig.4. Field photos showing trace fossils from the Middle Triassic Guanling Formation. A,  
1177 Horizontal *Archaeonassa* (arrowed); bed 9, SSK; B, *Arenicolites*; bed 2, XDP; C,  
1178 *Dikoposichnus*; bed 34, SSK; Note the two black arrows indicating the single imprints made  
1179 by animal limbs. White arrow indicates direction of movement of the trace maker. D–E,  
1180 Enlargement of *Diplocraterion* isp. from bed 42, SSK. Note the paired tube with spreiten,

1181 characterizing *Diplocraterion*. F, Dense *Diplocraterion* isp. preserved on thin-bedded  
1182 carbonate mudstone, bed 42, SSK; G, *Megagraption irregulare*, bed 42, DWZ.

1183  
1184 Fig. 5. Field photos showing trace fossils from the Middle Triassic Guanling Formation. A,  
1185 *Palaeophycus*, bed 172, XDP; B, *Planolites*, bed 171, SSK; C, *Rhizocorallium* isp.; bed 168,  
1186 XDP; D, *Rhizocorallium commune*, bed 71, XDP. E, *Rhizocorallium commune*, bed 70, DWZ.  
1187 F, detail showing the faecal pellets in marginal tubes of *R. commune*. G, *Sinusichnus* isp., bed  
1188 40, XDP. Note the Y-shaped (white arrow) and T-shaped (black arrow) branchings in burrow  
1189 system. H is a sketch of G showing the overall morphology of *S. isp.*.

1190  
1191 Fig. 6. Field photos showing trace fossils from the Middle Triassic Guanling Formation. A,  
1192 *Spongliomorpha* isp., bed 9 SSK. Note the longitudinal scratch marks on burrow surface  
1193 (white arrows). B, *Taenidium barretti*, bed 35, SSK; C, *Thalassinoides suevicus*, bed 34, SSK.  
1194 Note the swelling and Y-shaped branching in *Thalassinoides suevicus* (arrows). D, *Undichna*  
1195 *unisulca*, Bed 105, DWZ; E, *Zoophycos* isp. ?; Guangling Formation, Boyun; F, *Zoophycos*  
1196 isp., DWZ; Coin is 2.5 cm in diameter, DWZ.

1197  
1198 Fig. 7. Burrow size measurements of commonly occurring trace fossils at Luoping, Yunnan  
1199 Province. A, *Planolites*, bed 171, XDP; B, large sized *Rhizocorallium commune*, isp., bed 36,  
1200 XDP; C, small sized *Rhizocorallium* isp., bed 168, XDP; D, *Thalassinoides suevicus*, Bed 34,  
1201 SSK.

1202  
1203 Fig. 8. Statistical analysis of pyrite framboids from fossil beds of the Luoping Biota. A, SEM  
1204 photo showing pyrite framboids from marly carbonate mudstone, bed 15, SSK section. Note  
1205 the abundant pyrite framboids (black arrows) of similar sizes occurring densely. B, Histogram  
1206 showing the distribution of diameters of pyrite framboids for rock samples from the same bed.  
1207 C, SEM photo of framboid pyrite from carbonate mudstone, bed 33, SSK. D, Histogram  
1208 showing the diameter distribution of pyrite framboids for rock samples of the same bed MD =  
1209 mean diameter; SD = standard deviation.

1210  
1211 Fig. 9. Burrow size comparison of typical ichnotaxa from latest Permian to Middle Triassic. A,  
1212 *Planolites*; B, *Rhizocorallium*; C. *Thalassinoides*; Changh.: Changhsingian; Grie.:  
1213 Griesbachian; Die.: Dienerian.

1214

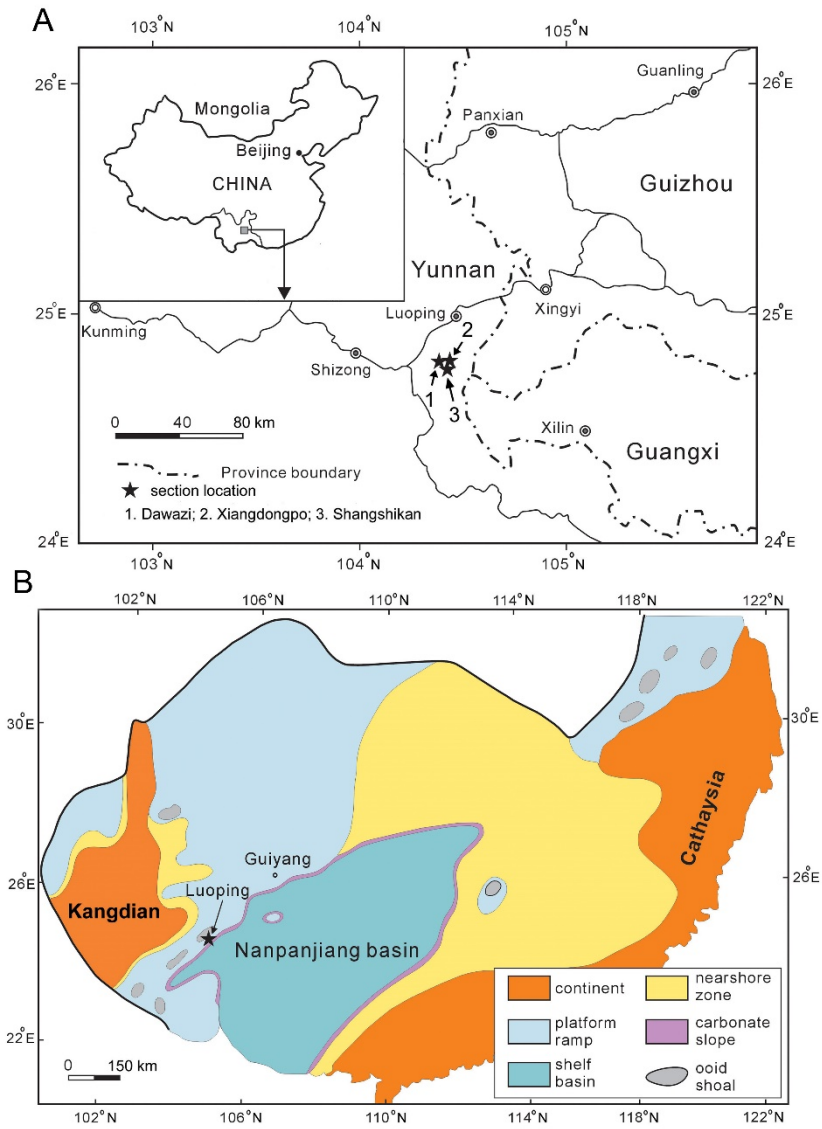


**Figure 1**

1215

1216

1217

1218

1219

1220

1221

1222

1223

1224

1225



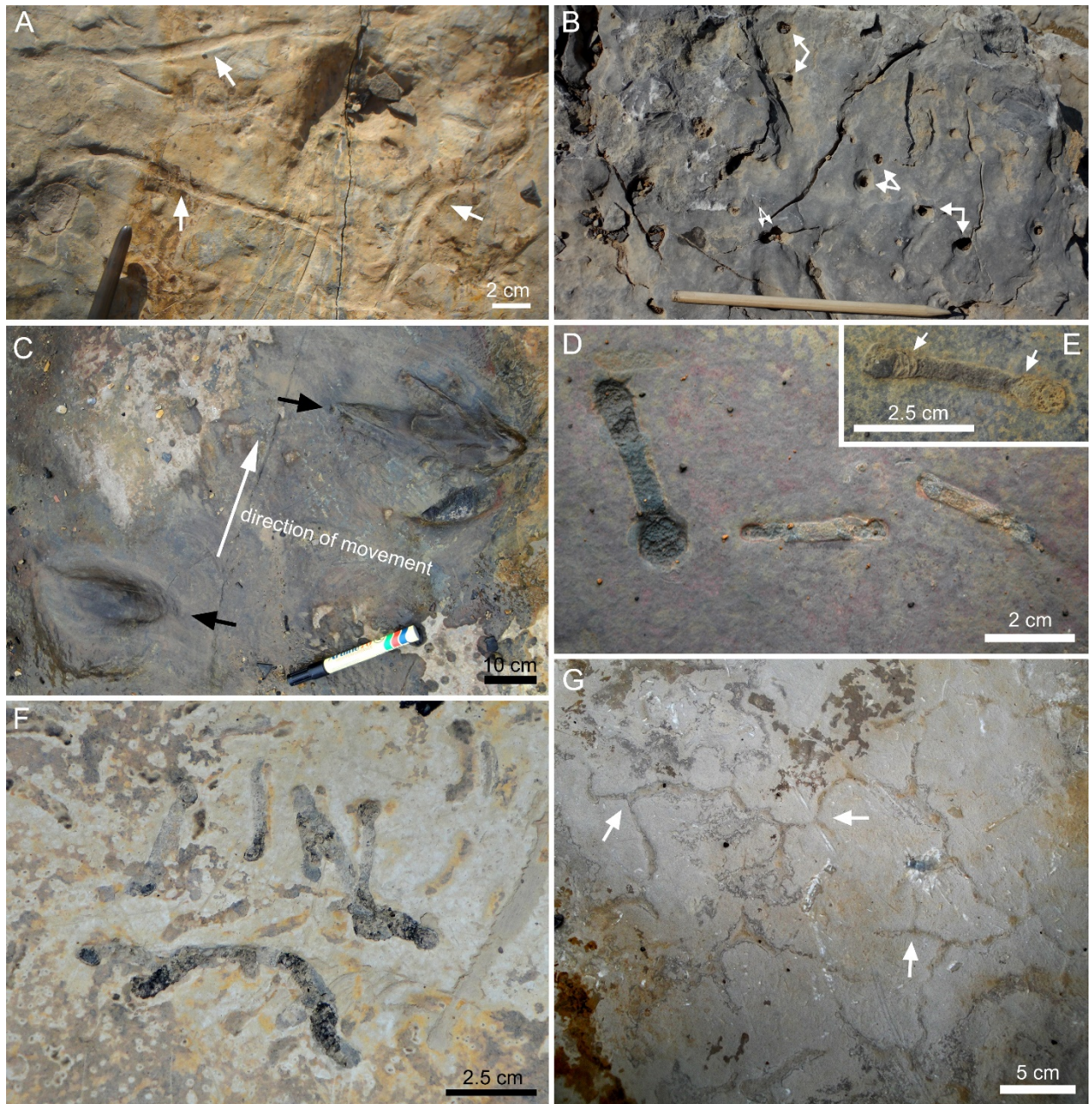


Figure 4

1226

1227

1228

1229

1230

1231

1232



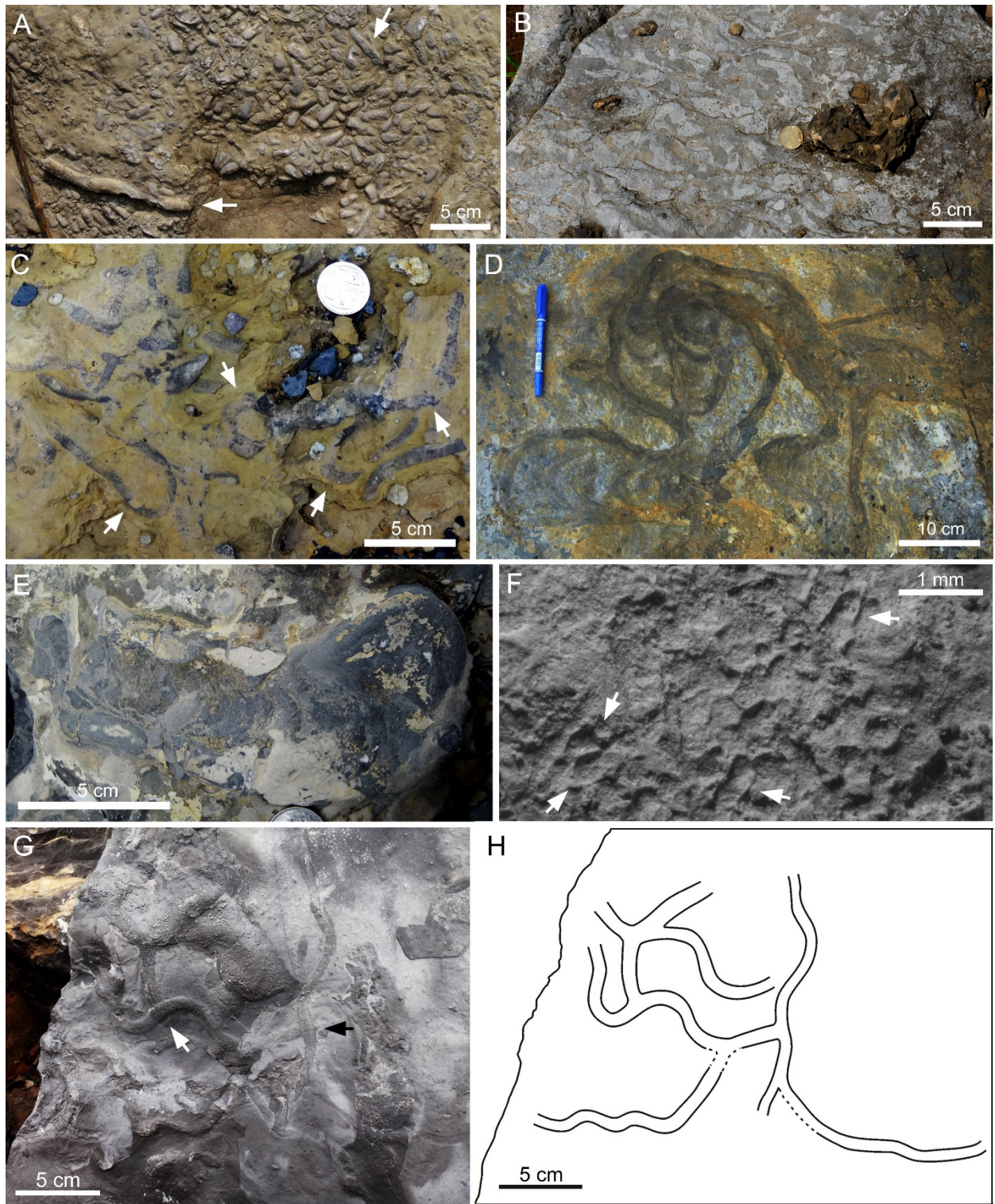


Figure 5

1233

1234

1235

1236



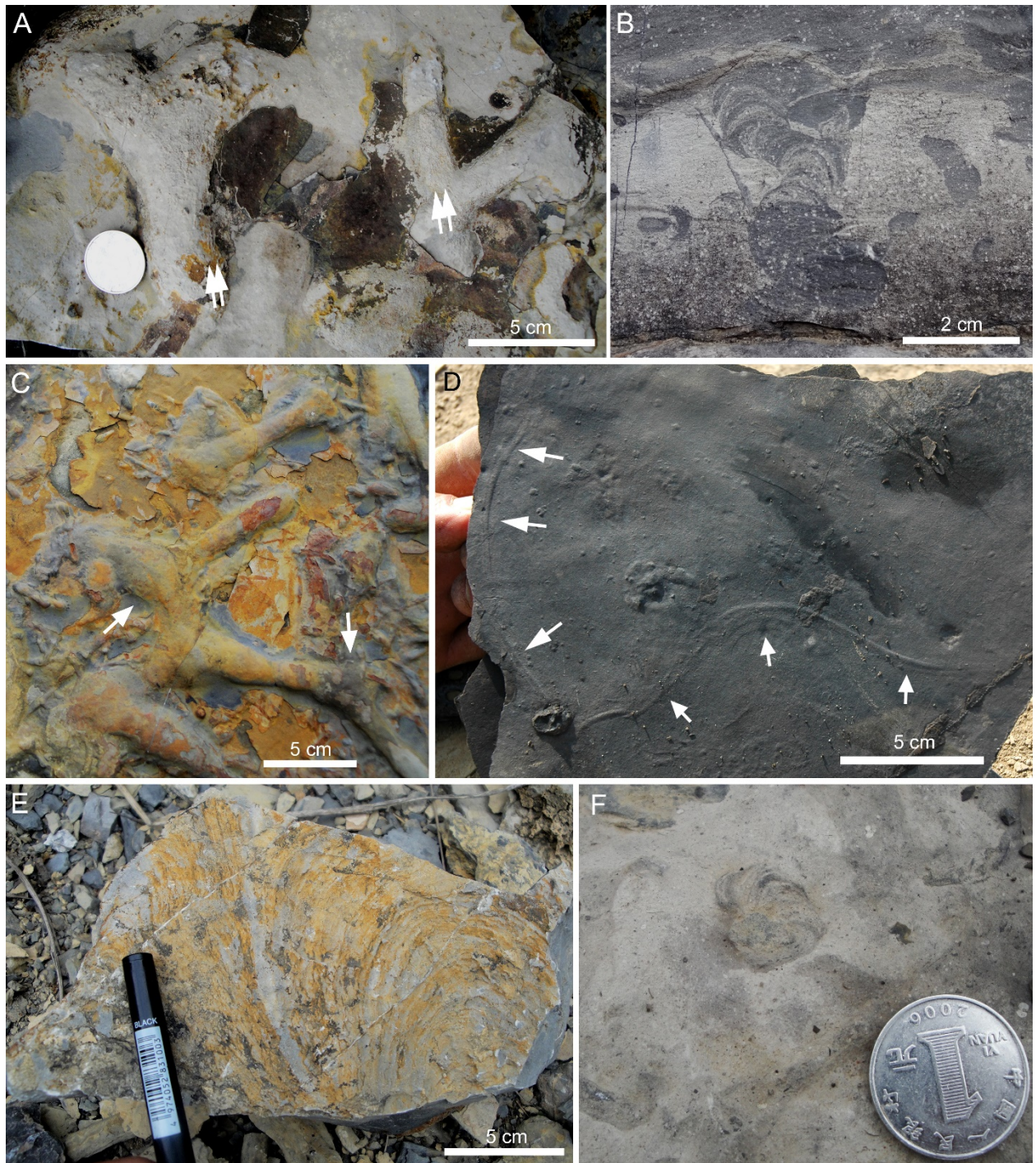


**Figure 6**

1237

1238

1239

1240